A methodology for designing 2.45 GHz wireless rectenna system utilizing Dickson Charge Pump with Optimized Power Efficiency.

by

Prince Mahdi Masud

A thesis
presented to the University of Waterloo
in fulfillment of the
thesis requirement for the degree of
Master of Applied Science
in
Electrical and Computer Engineering

Waterloo, Ontario, Canada, 2013

Author's Declaration

I hereby declare that I am the sole author of this thesis. This is a true copy of the thesis, including any required final revisions, as accepted by my examiners

I understand that my thesis may be made electronically available to the public.

Abstract

In the present thesis, I have proposed methodology of two stages Dickson charge pump, which is capable of harvesting energy at 2.45 GHz RF signal to power any low powered device. Presented design uses a simple and inexpensive circuit consisting of four microstrip patch antennas, some zero-bias Schottky diodes, Wilkinson power divider and a few passive components. Circuit was fabricated on a 60 mils RO4350B substrate (ε_r=3.66), with 1.4 mils copper conductor. Demonstration showed the charge pump provides a good performance, as it drives the low powered devices with as low as 10dBm input power at 1m away from the energy source. Thesis paper will present design techniques illustrated with data obtained on prototype circuits.

The objective is to wirelessly gather energy from one RF source and convert it into usable DC power that is further applied to a set of low power electronic devices. Radio Frequency Identification (RFID) tag system could also be improved using this method. RF-to-DC conversion is accomplished by designing and characterizing an element commonly known as a Rectenna, which consists of an antenna and an associated rectification circuitry. The rectenna is fully characterized in this dissertation and is used for charging low powered devices.

Acknowledgments

I wish to thank my family for all their support throughout my education, specifically, my mother. I would also like to thank Dr. Safieddin Safavi-Naeini for inspiring me to continue on this wireless power transmission research and to play with electromagnetics. Special thanks to my loving wife for sacrificing the best moments of her newly married life. Also, I am very grateful to my manager, Adnan Khan at Research In Motion to give me proper permission for testing my antenna and rectifier circuits using RIM's testing facility.

Finally, I would like to thank my honorable professor, Dr. Omar Ramahi, my thesis reviewers as well as the GRAD students from the CIARS Group for attending in the seminar and forwarding valuable comments and suggestion for my future research.

Table of Contents

List of Figures

List of Tables

Chapter 1: Introduction

1.1 Motivation

21st century's technological revolution has provided us lot of devices like cell phone, tablets, laptops, portable electronic devices that are now integral part of our life. Using electromagnetic waves, these devices transfer tons of data; keep us updated with rapid changing world.

While new technologies are moving towards portability, onboard power supply became important requirement. Batteries allowed us more portable systems, less hassle with wires. Using this wireless power transmission system concept, we can get rid of bulky cords, and the complications associated with the power interconnections.

Nevertheless utilizing transmission power system broadcasted from base stations will be an efficient way while devices will be under Wi-Max, Wi-Fi or cellular coverage. It will reduce portable device's weight since batteries are heavier part of modern devices. Modern days, electronic circuits are consuming less power, also these are improving day by day, which extends battery life in a significant way. So, in near future, battery less portable devices will become obvious. In this thesis the idea of battery-less portable devices will be explored, and also the notion of wireless power charging will be presented and discussed.

Within microwave radio spectrum, ISM (Industrial, Scientific and Medical) bands are very popular and widely used in wireless LAN networks (IEEE 802.11), wireless telephones and Bluetooth devices which are commonly used in different environments such

as at work, in schools and laboratories, even inside homes. Within this frequency band, efficiencies of microwave components are also very high.

The motivation for this thesis work arises to fulfill power charging requirement of handheld small electronic devices at RF frequencies while devices will be under coverage of WLAN and/or Cellular coverage. Similar kind of wireless systems are widely used for the wireless power transmission concept for RFID tags. Passive RFID tags usually operate without separate external power source and by converting the RF signal to DC voltage, the tag supplies necessary power.

So for starters, microwave circuit of a rectenna system that gathers the RF power from source and transforms it to DC power will be designed, fabricated, and extensively analyzed. Chapter 2 will focus on general theoretical background that is required to clearly understand the proposed system. Chapter 3 will present in full detail the design elements used for the development of the wireless power receiver system. Chapter 4 presents all the experimental lab results obtained from the implementation and realization of the rectenna system. Finally, Chapter 5 gives the conclusions and future work proposals for the Wireless rectenna concepts.

1.2 Wireless Power Transmission History

According to early history, Heinrich Hertz started power transmission by radio waves and also demonstrated electromagnetic wave propagation in free space by using a complete system with a spark gap to generate high-frequency power and to detect it at the receiving end using parabolic reflectors at both transmitting and receiving ends of the system (1).

Nikola Tesla also performed experiments on power transmission using radio waves at the turn of the century. He was interested more in the broad concept of resonance and tried to apply the principle to the transmission of electrical power from one point to another without wires. By means of the alternating surges of current running up and down a mast, Tesla hoped to set up oscillations of electrical energy over large areas of the surface of the Earth, thus generate standing waves into which he would immerse his receiving antennas at the optimum points (1).

Tesla first attempted to transmit power wirelessly at Colorado Springs, Colorado, in 1899. He created gigantic coil in a large square building over which rose a 200-ft mast with a 3-ft diameter copper ball positioned at the top. Tesla coil was resonated at a frequency of 150,000 Hz and fed with 300 kW of low- frequency power obtained from the Colorado Springs Electric Company. When the RF output of the Tesla coil was fed to the mast an RF potential was produced on the sphere that approached 100,000,000 V, according to Tesla. However, no significant record was found about radiated power into space and whether any significant amount of it was collected at a distant point.

Not until the early 1930's was another experiment performed to transmit power without wires which was performed in the Westinghouse Laboratory by H.V. Noble, consisted of identical transmitting and receiving 100 MHz dipoles located about 25 ft from each other. No attempts were made to focus the energy, but several hundred watts of power were transferred between the dipoles (1).

Knowledgeable people realized that efficient point-to-point transmission of power depended upon concentrating the electromagnetic energy into a narrow a beam, during the first fifth years of this century. This was the main reason for the lack of serious interest in wireless power system. The only way it could be done, by using electromagnetic energy of very short wavelengths and assemble energy over large diameters via optical reflectors or lenses. For the first thirty five years of this century, it didn't provide even a few miliwatts of energy at these wavelengths. Till the development of magnetron, sufficient powers are not available for experimental work in communication and radar systems. Afterwards, modern history for free-space power transmission started from RFID tags to unmanned vehicles.

1.3 Classification of wireless systems

A wireless system normally considered the communication of information between two points without the use of a wired medium. This wireless medium could be sonic, infrared, optical, or radio frequency energy. In early days, television remote controllers used ultrasonic signals. It has very low data rates and poor exemption to interference. Thus

it makes a poor option for modern applications. Infrared signals can purvey moderate data rates, but the fact is infrared radiation is easily stopped by even a tiny obstructions limits. It is used in low range indoor applications like remote controllers and local area data links. Similarly, optical signal propagating in an unobstructed environment and in line-of-sight path can transfer moderate to high data rates. It cannot be used in a place where dust, foliage, or fog can obstruct the signal. Therefore, most modern wireless systems depend on RF and microwave signals, normally in the UHF (100MHz) to millimeter wave (30GHz) frequency range. Therefore, spectrum crowding and need for higher bandwidth. The direction is to use higher frequencies, in order that the majority of present wireless systems operate at frequencies range from about 800MHz to a few gigahertzes. RF and microwave signals give wide bandwidths. It has the added benefits of being able to pervade fog, dust, foliage, and also buildings and vehicles partly. One way to classify wireless systems is according to the nature and placement.

For the users, a single transmitter convey with a single receiver in a point-to-point radio system. These systems commonly use high-gain antennas in fixed positions to maximize received power and minimize interference with other radios, which may be operating nearby in the similar frequency range. Point-to-point radios are usually used for dedicated data communications by utility companies, for connection of cellular phone sites to a central switching office. Most common examples are commercial AM and FM broadcasting radio and broadcast television. Adhoc (point to point) systems concede simultaneous communication between particular users.

1.4 Wireless Local Area Networks

Wireless local area networks (WLANs) are now used every day to establish connections between various handheld devices and with internet. Within few meter distance, typical use is in hospitals, office buildings, and factories, even at home. In absence of obstacles and using high gain antennas, few miles range can be obtained at outdoor. Wireless networks are especially useful when it is impossibly or prohibitively expensive to place wiring in or between buildings, rural areas or vast metropolitan areas. Cellular phones now became very popular among all ages of people, is a good example for wirelessly connected most useful devices.

Industrial, Scientific, and Medical (ISM) frequency bands (both 2.4 GHz and 5.8 GHz) are mostly used in all kind of commercial WLAN products all over the world. Using either frequency- hopping or direct-sequence spread spectrum techniques on IEEE standard 802.11, current WLAN products are capable to send data from 1Mbps to 1.3 Gbps (802.11AC), which are very convenient, flexible and faster than any ethernet cable connections. Significant amount of power is transmitted from WLAN access point which can be utilized to recharge connected low power devices over period.

1.5 RFID

Radio Frequency Identification (RFID) systems are commonly used for inventory tracking, shipping, personal security access, auto toll collection and other functions.

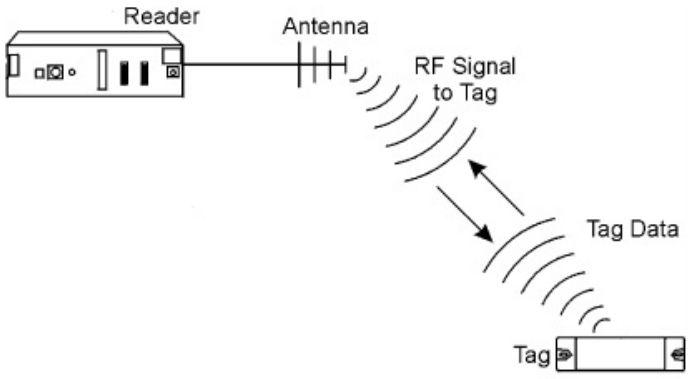

Figure 1 Base microwave RFID Systems

Wireless rectenna system that has been proposed in this present dissertation, is an improved version of legacy RFID. The proposed wireless rectenna system and an RFID system are similar because both systems collect energy from the environment. Finally both use rectennas as the transducer element between RF energy and DC power. But propose wireless rectenna system is centered on the far-field transmission region, whereas legacy RFID is located in the near field region. Main idea behind energy harvesting is utilizing the transmitted wireless power from the RFID reader to power the tag itself. On board power supply is no longer needed because of this advantage which reduces weight, size, cost, and battery replacement hassle. On the other hand, complexity of design and low received power efficiencies are some of the disadvantages.

The current techniques for an energy harvesting device are based upon an antenna and some flavor of energy harvesting circuitry. This is very sound in theory but the resulting DC voltage is not high enough to handle many devices. For example, energy harvesting from a 100kW radio station at frequency 954 kHz with a 6-stage Dickson charge pump can only produce 520 mV DC at 15 kilometers away. The circuit is only able to harvest 60.2μJ in half an hour, which is only high enough to charge very low powered devices. (2)

RFID tags are mainly categorized as active and passive device. Active tags are powered by internal means such as battery, and passive tags harvest RF energy. Active tags are bulkier and more expensive, due to the power source, than their passive counterparts. Passive tags which only require less energy harvesting circuitry typically cannot provide the same power and range capabilities as active tags, so their applications limited for shorter range and simple communication. For example, a passive tag should not be used when any complicated operations on a microcontroller must be performed on tag since the microcontroller must draw higher current. A passive tag often only powers a simple microcontroller to flip a switch, creating an open-circuit or short-circuit to vary the antenna feed reflection coefficient. The reader can identify the tag's ID based on the wireless signal reflected from the tag being a positive or negative reflection. Since the microcontroller only needs to flip a switch, the microcontroller draws very little power and can run off a low DC voltage. In addition, since reader's RF signal is modulated and backscattered, the tag does not need to provide the antenna with its own RF signal to relay the information back to the reader. This application is ideal for an energy harvesting circuit.

According to some discussion, passive tag has three main sections: an antenna, an energy harvesting circuit, and some microcontroller. Charge pump used in the energy harvesting circuitry, converts an AC signal to a DC voltage that supplies power to the microcontroller. Various charge pump topologies are currently available such as the Buck converter, Dickson method and the Cockcroft-Walton Voltage Multiplier. These all have their benefits and tradeoffs, these topologies are comprised of several stages of shunt capacitors connected with series diodes. Each stage has a capacitor that holds charge. Theoretically more capacitor and diode stages can increase voltage output, but it also depends on diode's threshold voltage.

Another important element for RFID and wireless power harvesting is antenna. For most RFID tags, the patch or printed antenna is commonly used for its low-profile design as well as having about 7 dB gain and a fairly large half power beam width of approximately 60 degrees. Its high gain over a large beam width makes it a strong candidate for energy harvesting since it not highly directional but has a gain five times that of an isotropic antenna.

Last but not the least; the microcontroller is a crucial part of the RFID tag which sets the required DC voltage and power. In low power RFID applications, most microcontrollers will have DC operating voltages around 1 to 3.5 V and the current draws from 0.5 μA to 100 μA during peak power operation.

1.6 NFC Charging

NFC charging or wireless charging became hot topics and requirements for almost all cellular carriers to charge device within near field region which uses inductive charging method. Though far field charging is still not widely used and capacitive charging is the basic structure/requirement for far field charging. Nexus 4 wireless charger from Google, Nokia's wireless charging plate and JBL Powerup Wireless Charging Speaker are few of renowned NFC devices that are currently available in market.

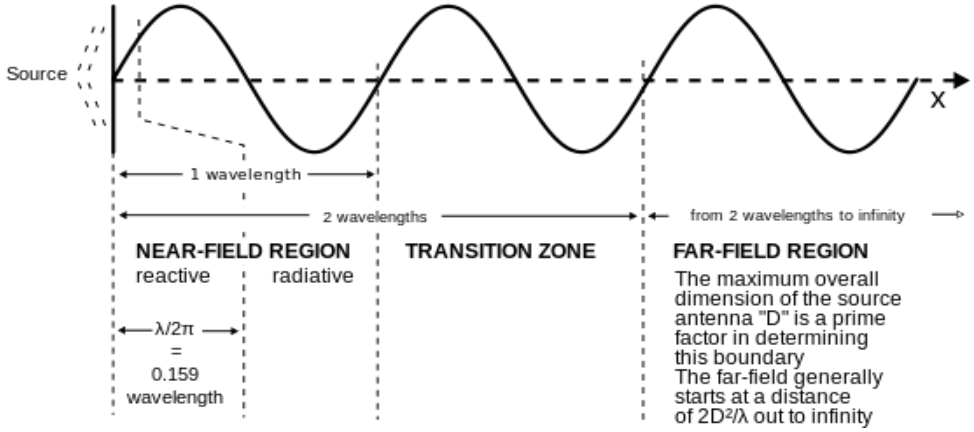

Figure 2 Antenna Field Regions (2)

Though these technologies are very demanding, sometimes during lab test we have realized there are some interference between their transmitters and regular Wi-Fi signal when they are both on same 2.4GHz channel. Also, these NFC chargers are not convenient for mobility. So, to get rid of this interference, rectifying only Wi-Fi received signal is best option as well as cost effective since we will not need to design an extra transmitting antenna. We can just utilize the transmitting signal coming from base stations within Wi-Fi or cellular coverage areas. To achieve maximum efficiency, we will have to optimize rectifier circuits at particular distance, phase as well as frequency.

Chapter 2: Theoretical Background

Basic theory for single patch antenna was presented in this section with an investigation of the theory behind charge pumps, through explicit equations.

2.1 Basic Principles

Three steps define for wireless power transmission system:

- DC power is converted into RF signal power.
- RF power is then propagated through space to some distant point
- Transmitted power is collected as well as converted back into DC power at receiving point.

So, overall WPT efficiency depends on individual efficiencies associated with the three steps or elements of the system.

Due to the development of CMOS technology as well as low powered Integrated Circuits (IC's), power saving becomes possible in large amount.

Transferring energy from transmission point to receiver point has following features:

- Massless media is required between the source and consumption point of energy.
- Energy is transferred at the velocity of light
- Energy transfer direction can be rapidly changed

Due to earth's atmosphere, little energy is lost in the at longer microwave wavelengths.

2.1.1 Free space transmission

The size and expense of these apertures has a direct relationship to the used wavelength, transmission distance, and desired transmission efficiency. Goubau and others (3) have derived the following relationship between the aperture to aperture efficiency and a parameter τ given in figure 3.

$$\tau = \sqrt{(A_t\, A_r)/\lambda D}$$

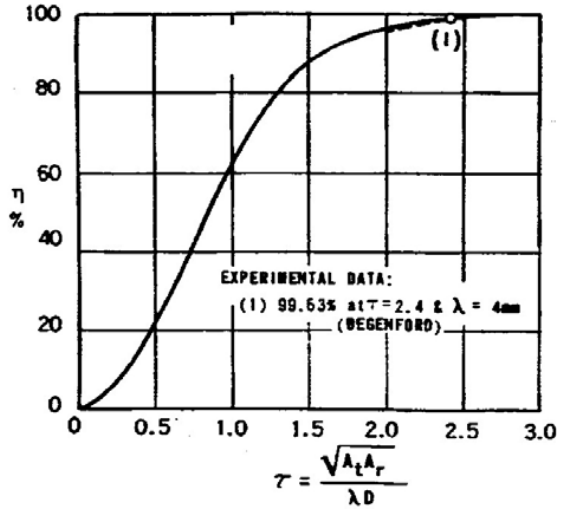

Figure 3 Transmission efficiency as the function of parameter tau.

Where,

A_t = Transmitting aperture area

A_r = Receiving aperture area

λ = Transmitted power wavelength

D = Separation distance between two apertures

When the reception area may be limited and where a particular intensity of the incident microwave illumination is desired. Under those circumstances we may use:

$$P_{r=} A_t P_t / \lambda^2 D^2$$

Where,

P_r = Power density at the center of the receiving location

P_t = Total radiated power from the transmitter

A_t = Total area of the transmitting antenna

D = Distance between the apertures

At the receiver site, to achieve a desired value of P_r while being constrained by a fixed transmitted power P_t, transmitting aperture area varies as the inverse square of the wavelength of the radiation.

2.1.2 Radio Link and Friis equation

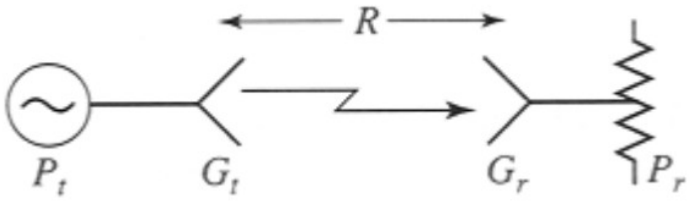

Figure 4 Block diagram for a general radio link

A general radio link is shown in above figure, where the transmit power is P_t, the transmitter antenna gain is G_t, the receiver antenna gain is G_r, and received power which is delivered to a matched load is P_r. The transmit and receive antennas are separated by the distance R.

By conservation of energy, the power density S_{avg} radiated by an isotropic antenna at a distance R is given by:

$$S_{avg} = \frac{P_t}{4\pi R^2} \text{ W/m}^2$$

P_t is the power radiated by transmitting antenna. This result is deduced from the fact that we must be able to recover all of the radiated power by integrating over a sphere of radius R surrounding the antenna; since the power is distributed isotropically, and the area of a sphere is $4\pi R^2$. If the transmit antenna has a positive, then radiated power density could be calculated by multiplying by the directivity, since directivity is defined as the ratio of the actual radiation intensity to the equivalent isotropic intensity. Also, we can include the radiation efficiency factor if transmitter antenna has losses. Thus, the general expression for the power density radiated by an arbitrary transmit antenna is

$$S = \frac{P_t G_t}{4\pi R^2}$$

Using this power density equation and the concept of effective aperture area defined above, we can obtain the following expression for the received power:

$$P_r = S_{avg} A_e = \frac{P_t G_t A_e}{4\pi R^2}$$

2.1.3 Free Space Path Loss

In radio communication, free-space path loss (FSPL) is considered as the loss in electromagnetic wave's signal strength that will propagate from a line-of-sight path through free space, without any near-by obstructers to cause reflection, refraction or distortion. Gain of antennas either transmitter and receiver or hardware losses are not considered here, more details could be found in link budget calculation. (3)

The expression for FSPL actually encapsulates two effects. First effect is spreading out of electromagnetic energy in free space which is determined by the inverse square law:

$$S=P_t \frac{1}{4\pi d^2}$$

Where

S = Power per unit area or power spatial density (in watts per meter-squared) at distance, d

P_t= Total power transmitted (in watts).

Note that there is no a frequency-dependent behavior.

The second effect is that of the receiving antenna's aperture, which describes antenna's power receiving capacity from an incoming electromagnetic wave. For an isotropic antenna, this is derived by

$$P_r = S\frac{\lambda^2}{4\pi}$$

Where P_r= received power. Note that this is entirely dependent on wavelength, which is how the frequency-dependent behavior arises.

By combining above two effects, total free-space path loss can be derived, which becomes proportional to square of the distance between the transmitter and receiver, and proportional to the square of radio frequency. For far field region, this equation is only valid where spherical spreading can be assumed.

The equation for FSPL = $\frac{P_t}{P_r} = (\frac{4\pi d}{\lambda})^2 = (\frac{4\pi df}{c})^2$

In terms of dB: FSPL (dB) = $10 \log_{10} \left(\frac{4\pi df}{c}\right)^2$

$$= 20 \log_{10}(\frac{4\pi df}{c})$$

$$= 20 \log_{10} d + 20 \log_{10} f + 20 \log_{10}(\frac{4\pi}{c})$$

$$= 20 \log_{10} d + 20 \log_{10} f - 147.55$$

Where

λ= signal wavelength (in meters),

f= signal frequency (in hertz),

d = distance from the transmitter (in meters),

c = speed of light in a vacuum, 3×10^8 meters per second.

In this design, 2.45GHz, ISM band has been chosen, since it has low atmospheric attenuation (5). As far as 2 m distance, there should be around -43dBm free space loss.

Since wavelengths for 2.4 GHz phones are even shorter than 900 MHz wavelengths and consequently cover a room quicker. Though 5.8 GHz band signal cover an area even faster, transmitting signals at a higher frequency needs more power.

2.2 Rectenna Design

The term rectenna is commonly denoted as rectifying antenna at microwave power transmission system, basically combines the functions of an antenna and high efficient rectifier circuits. In its simplest form, rectenna consists of a collection of receiving antenna elements that feeds a low pass filter circuit terminated in some rectifying diodes. Rectenna has many desirable characteristics, including followings:

1. In its pure form, the aperture collection efficiency is independent of the illumination density distribution across the aperture regardless of the size of the aperture.
2. An overall conversion efficiency from incident microwave power to DC power output, could be achieved over 85%.
3. Rectenna can be designed for any desired frequency to harvest RF power which is very cost effective and easy to design.

2.2.1 Microstrip patch antennas

Microstrip patch antenna consists of a conducting patch of any planar or non- planar geometry on one side of a dielectric substrate with a ground plane on the other side. Rectangular and circular patch antennas are widely used which have light weight with low fabrication cost. Micro strip patch antenna has a typical gain between 5 and 6 dB with 3 dB beam width between 70◦ and 90◦.

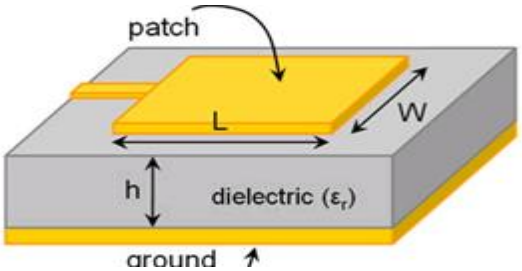

Figure 5 microstrip rectangular patch antenna

As shown in above figure, basic antenna element is a strip conductor of dimensions L × W on a dielectric substrate of dielectric constant, ε_r and substrate thickness,*h* backed by a ground plane. Free space wavelength, λ is normally considered.

For an efficient radiator, resonance frequency is controlled by length of Microstrip Patch Antenna, L and dielectric constant $f_{10} = \frac{C}{\sqrt{\epsilon_r}}(\frac{1}{2L})$

Width of patch antenna, $W = \frac{v_o}{2f} \sqrt{\frac{2}{\epsilon_r+1}}$

Input impedance of the patch can be derived by following equation:

$$Z_A = 90 \frac{\epsilon_r^2}{\epsilon_r - 1} (\frac{L}{W})^2$$

Microstrip antenna feed line run deeper into patch a certain distance (Δx) to match with antenna Impedance calculated above:

$$Z_o' = Z_A \cos^2(\frac{\pi \Delta x}{L})$$

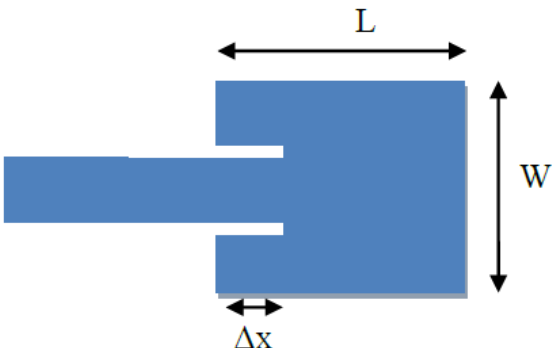

Figure 6 Patch antenna design example layout with Inset

After solving for Δx, trace must enter the patch antenna to match the antenna with 50 Ohm trace. The factor $\cos(\frac{\pi x f}{L})$ arises due to electric field variations for the dominant mode. Although the feed point can be selected anywhere along the patch width, it is better to choose $y_f = \frac{W}{2}$ if $W \geq L$ so that TM_{0n} (n odd) modes are not excited along with the TM_{10} mode.

The radiation efficiency, $\in_r$ is defined as the ratio of the radiated power P_r to the input power P_{in}, that is,

$$\in_r = \frac{P_r}{P_{in}}$$

The input power gets distributed in the form of radiated power, surface wave power, and dissipation in the conductors and dielectric. Therefore, above efficiency can be expressed as

$$\in_r = \frac{P_r}{P_r + P_c + P_d + P_{sur}}$$

Here, P_d is the power lost in the lossy dielectric of the substrate, P_c is the power lost due to the finite conductivity of metallization which is also called copper loss, P_r is the

power radiated in the form of space wave, and P_{sur} is the power lost in the form of power carried away by the surface waves.

2.2.2 Rectifier Basic

A rectifier is a circuit that converts the RF signal into a zero frequency (DC) signal with time and frequency-domain signals as shown in figure 7. The rectifier is commonly used for automatic gain control (AGC) circuits or power monitor circuits, etc. High frequency diodes are heart of the rectifiers along with some passive components. To design efficient rectifier, designers mainly focus on diode's voltage sensitivity as well as overall rectifying efficiency of the diodes. Return loss from rectifier circuit is also a crucial factor during power harvesting to get maximum output power.

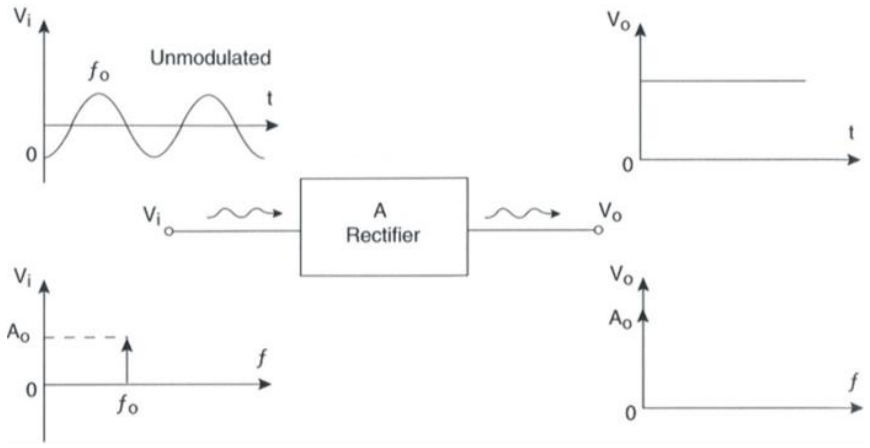

Figure 7 Time and Frequency Domain Signals for a Rectifier

2.2.3 Schottky Diode Fundamentals

Schottky diode is a metal-semiconductor contact formed between a metal and an n-doped or a p-doped semiconductor. In a metal-semiconductor junction, free electrons flow

across the junction from the semiconductor and fill the free-energy states in the metal. This flow of electrons creates a depletion or potential across the junction. The difference in energy levels between semiconductor and metal is called a Schottky barrier.

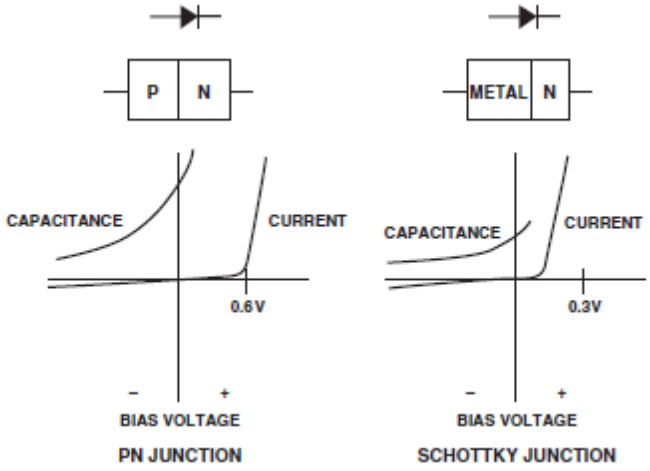

Figure 8 Schottky Diode Fundamentals

P-doped, Schottky-barrier diodes excel at applications requiring ultra-low turn-on voltage (such as zero-biased F detectors). But their very low, breakdown-voltage and high series-resistance make them unsuitable for the clipping and clamping applications involving high forward currents and high reverse voltages. Therefore, in this paper will focus entirely on n-doped Schottky diodes. (6)

Under a forward bias (metal connected to positive in an n-doped Schottky), or forward voltage, V_F, there are many electrons with enough thermal energy to cross the barrier potential into the metal. Once the applied bias exceeds the built-in potential of the junction, the forward current, I_F, will increase rapidly as V_F increases. Diodes which are made of silicon drop approximately 0.5 to 0.7 volts when forward bias whereas germanium diodes drop approximately 0.3 to 0.4 volts. When the Schottky diode is reverse biased, the

potential barrier for electrons becomes large; hence, there is a small probability that an electron will have sufficient thermal energy to cross the junction. The reverse leakage current will be in the nano-ampere to microampere range, depending upon the diode type, the reverse voltage, and the temperature. (6)

In contrast to a conventional p-n junction, current in the Schottky diode is carried only by majority carriers (electrons). Because no minority-carrier (hole) charge storage effects are present, Schottky diodes have carrier lifetimes of less than 100 ps. This extremely fast switching time makes the Schottky diode an ideal rectifier at frequencies of 50 GHz and higher. Another significant difference between Schottky and p-n diodes is the forward voltage drop. Schottky diodes have a threshold of typically 0.3 V in comparison to that of 0.6 V in p-n junction diodes. (7)

In general, a diode can be considered to be a nonlinear resistor with its I-V characteristic curve mathematically given by:

$$\boldsymbol{I}(V) = \boldsymbol{I_s}\ e^{(V/nV_t)} - 1$$

Where

$V_t = \frac{KT}{q}$ $\quad$ $(V_t = 25mV\ at\ T = 293K)$

$\boldsymbol{I_s}$ = Diode's saturation current

n = Ideality factor ($1 \leq n \leq 2$) which depends on the material and physical structure of the diode. For example, for a point-contact diode n = 2 whereas for a Schottky barrier diode, n = 1.2, etc.

Following figure is a sketch of diode's I-V characteristic curve, as described in above

equation.

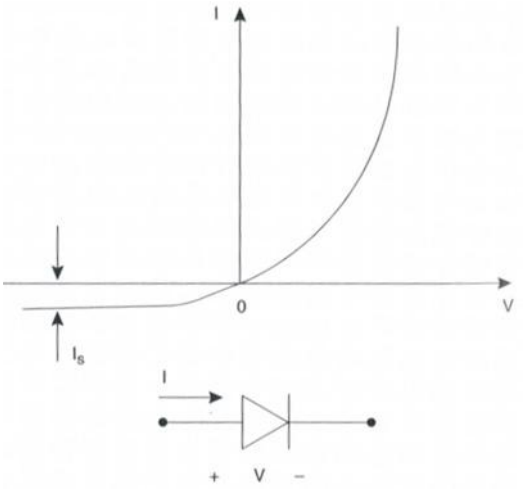

Figure 9 Diode's Voltage-Current Curves (8).

A typical equivalent circuit for the diode is shown below, C_J is the parasitic junction capacitance of the Schottky chip and R_S is the parasitic series resistance of the chip. L_P and C_P are package parasitic. R_J is the junction resistance of the diode, where RF power is converted into DC output voltage.

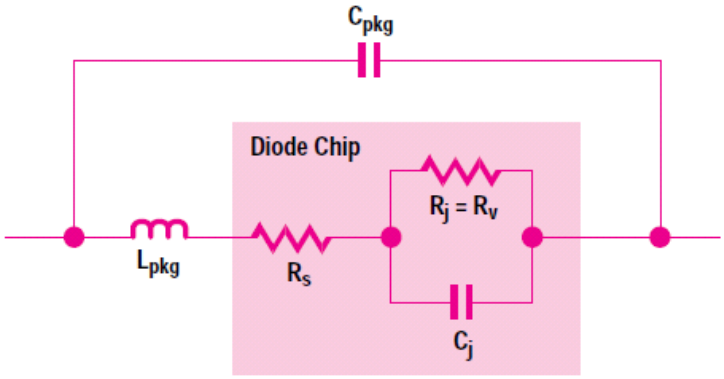

Figure 10 Linear equivalent circuit of Schottky Diode (15)

The diode’s junction capacitance shunts the junction resistance. Detected voltage is reduced because some of the input current flows through the capacitance and never reaches

the resistance where detection takes place. All incoming RF voltage should ideally appear across R_J with nothing lost in R_S for maximum output. The effect is more serious at higher frequencies because capacitance susceptance is proportional to frequency. Similarly, the effect is more serious for higher capacitance diodes. Capacitance effect on output voltage can be approximated by following equation, which accuracy is quite good for this purpose.

$$M = \frac{1}{1 + \omega^2 C_j^2 R_S R_j}$$

Where Ω= 2π times frequency

M = Multiplier for output voltage, V_o

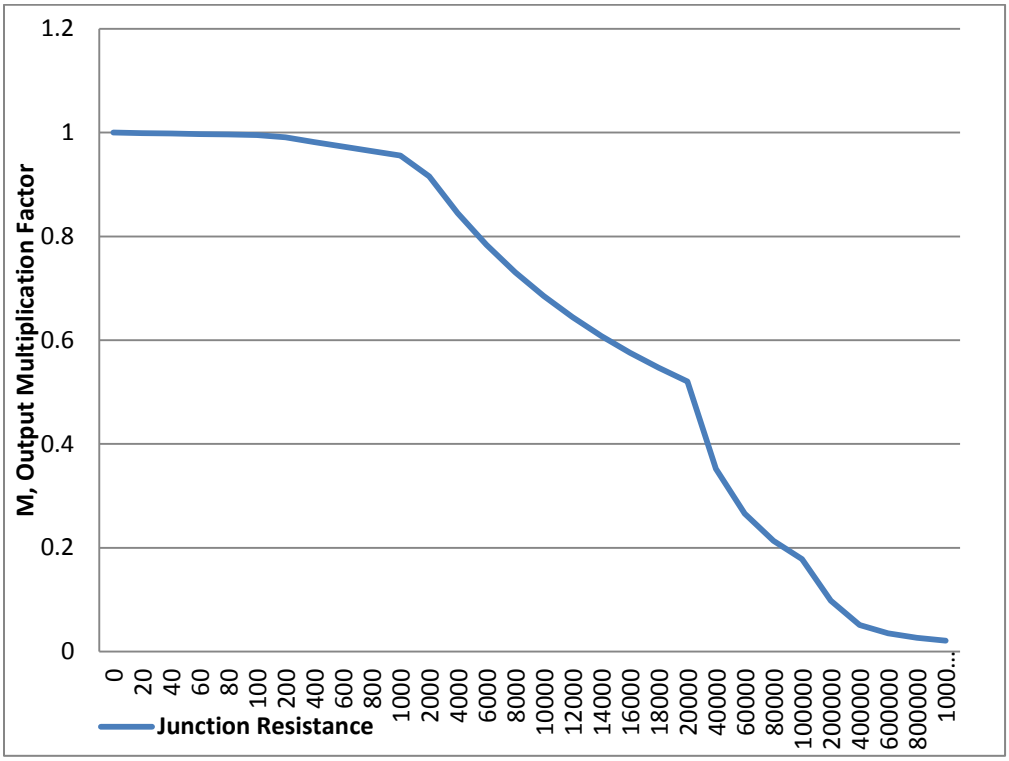

Figure 11 Output Multiplication Factor vs Junction Resistance (C_j=0.18pF, R_s=6Ω , f=2.45GHz)

Three different currents affect the junction resistance of a Schottky diode.

$I_c = \frac{V_o}{R_L}$ =circulating current generated by the rectification of RF power in the diode

I_o = externally applied bias current (if used), none for zero bias.

I_s = Diode's own saturation current, which is function of Schottky barrier height (4)

$$I_S = I_{so} \left(\frac{T}{T_o}\right)^{\frac{2}{n}} e^{\frac{-q\psi}{k}\left(\frac{1}{T}-\frac{1}{T_o}\right)}$$

where, T_o = 273°K =room Temperature.

I_{so}= saturation current measured at room temperature

Ψ = metal-semiconductor Schottky barrier height (energy gap)

So, $I_T = I_s + I_b + I_o$, in amperes

For small signal region of interest, where $I_c < I_s$, equation of junction resistance for zero bias

$$R_j = \frac{\partial V}{\partial I} = \frac{nkT}{qI_T} = \frac{nkT}{q(I_S+I_O)} = \frac{8.617X10^{-5}nT}{I_S+I_O} = \frac{0.028}{I_S}$$ at 300K

n = Diode ideality factor (emission coefficient)

k = Boltzmann's constant=1.38062 x 10^{-23} Joules/°k

q = Electronic charge=1.60219 x 10^{-19} Coulomb

T= Temperature in degrees kelvin.

2.2.4 Diode Impedance

From above linear equivalent circuit model of Schottky Diode, impedance can be found as follows:

First, we will derive impedance for junction resistance and capacitive reactance,

$$Y_{d1} = \frac{1}{R_j} + j\omega C_B \; ; \; Z_{d1} = \frac{1}{Y_{d1}} \; ; where, \omega = 2\pi f$$

After that, total diode impedance could be calculated as below,

$$Z_{d2} = \; Z_{d1} + R_s ; \; Y_{d2} = \frac{1}{Z_{d2}}$$

$$Y_{d3} = Y_{d2} + j\omega C_{pkg} \; ; \; Z_{d3} = \frac{1}{Y_{d3}}$$

$$Z_{diode} = \; Z_{d3} + j\omega L_{pkg}$$

2.2.5 Voltage Sensitivity

Detector diode's important performance characteristic is voltage sensitivity (γ). Basically, slope of the curve of output voltage vs input signal power is defined by this parameter (10).

V_{out} = voltage sensitivity (γ) x P_{in}

Neglecting parasitic and reflection losses, voltage sensitivity can be defined as $\gamma = \beta/(\frac{\partial I}{\partial V})$

where β is current sensitivity and has a theoretical value of 20 A/W.

Using the diode equation, $\frac{\partial I}{\partial V} = \frac{I}{0.0279}$

Therefore, $\gamma = \frac{0.558}{I}$

For zero bias detectors, $\gamma = \frac{0.558}{I_s}$

Using this simple analysis, perfect detector gives poor approximation of actual data on existing diodes. But considering diode junction capacitances, diode series resistance, load resistance and reflection loss, the analysis could be bring closer to reality.

Junction Capacitance and Resistance:

In most cases, the junction impedance associated with R_J and C_J is much greater than R_s, especially at low frequencies. However, at high frequencies, the junction impedance is reduced so that the RF power dissipated in R_s is comparable to that of the junction. Incorporating the errors of the diode capacitance and resistance on the current sensitivity, the voltage sensitivity for the zero bias diode becomes,

$$\gamma_1 = \frac{0.558}{I_s(1+\omega^2 C_j^2 R_S R_j)} = \frac{0.558}{I_s} M \qquad (1)$$

Where, $\omega = 2\pi f$, C_J is junction capacitance , I_s is diode saturation current , R_s is the series resistance, R_J is the junction resistance and M is output multiplication factor. So for higher sensitivity, we have to choose diodes that have low saturation current.

Load Resistance:

The diode resistance R_J at zero bias is not usually small compared to the load resistance, R_L. If the diode is considered as a voltage source with impedance, R_J feeding the load resistance R_L, the voltage sensitivity will be reduced by the factor $\frac{R_L}{R_L+R_j}$ or $\gamma_2 = \gamma_1 \frac{R_L}{R_L+R_j}$ (2)

When the ratio of diode resistance to load resistance is small, $\gamma_2 = \gamma_1$. This is a common condition for biased detectors. However, diode resistance is usually not small compared to load resistance at zero bias. For a high load resistance value, such as 100KΩ, the sensitivity, γ is inversely related to saturation current.

Reflection Loss:

Moreover voltage sensitivity is also reduced by reflection losses in diode's matching circuit. In Figure 10, the package capacitance C_{pkg} and package inductance L_{pkg} can be used to determine the packaged diode reflection coefficient. When this diode terminates at 50Ω system, the reflection coefficient ρ becomes:

$$\rho = \frac{Z_D - 50}{Z_D + 50}$$

Where Z_D is a function of frequency and package parasitic. In matching network's absence, the voltage sensitivity can be calculated as:

$$\gamma_3 = \gamma_2 (1 - \rho^2) \qquad (3)$$

The chip, package and circuit parameters all combine to define optimum voltage sensitivity for a given application. Using the voltage sensitivity analysis described above, we hoped to produce an optimum, low cost, manufacturable part in the shortest time possible. As a

result, for higher sensitivity, designing a good matching network, voltage sensitivity can be improved.

Overall Voltage Sensitivity:

When rectifier circuit will be perfectly matched with input circuit and there will be no or negligible return loss (ρ), ratio of diode resistance to load resistance is very small and circuit's output multiplication factor very close to 1, then using above equation 1, 2 and 3; we can derive that voltage sensitivity for overall rectifier circuit which is inversely related to saturation current. Thus to design a higher sensitive rectifier circuit, we have to choose a diode with a very low saturation current.

Chapter 3: Design Elements

3.1 Microstrip Patch Antenna Design

Typically antenna gain is between 6 to 15 dBi, though higher values narrows pattern more. Since we will design a far field antenna which uses capacitive coupling, has longer range but it is prone to Water & Metal. To simulate microstrip antenna, recommended simulation technique is electromagnetic full-wave simulations which have been performed using ADS.

Operating frequency(f_o)	2.45GHz	Power radiated (Watts)	0.0007
Width of single patch(W)	40.11mm	Effective angle(deg)	0.41 sterdian
Length of single patch(L)	31.60mm	Directivity(dB)	9.4735
Height	60 mils	Gain(dB)	8.1291
Distance between elements	0.5λ	E(theta)	144.2
Feed line Width	3.28mm	E(phi)	325.8
Dielectric Constant(ϵ_r)	3.66	Metallization Thickness	35μm
Input Impedance(edge)	209.7Ohm	Copper Conductivity	4.7×10^7(s/m)

Table 1 Patch Antenna Parameters

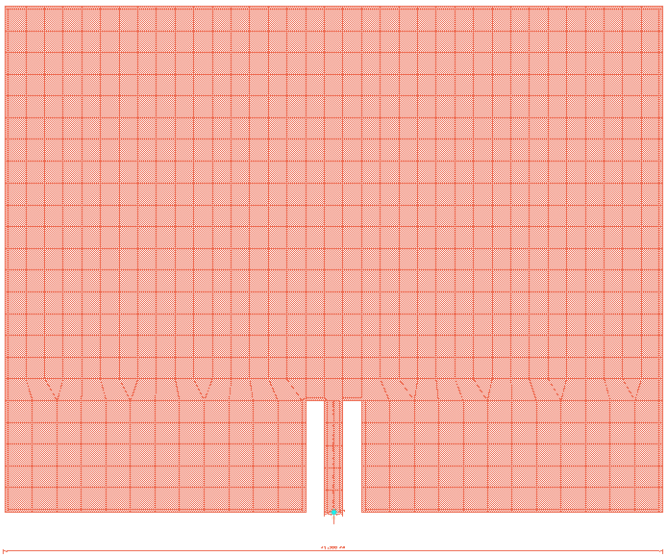

Figure 12 Single Microstrip Patch Antenna Layout on ADS

Return loss for single patch antenna has shown below from ADS simulation:

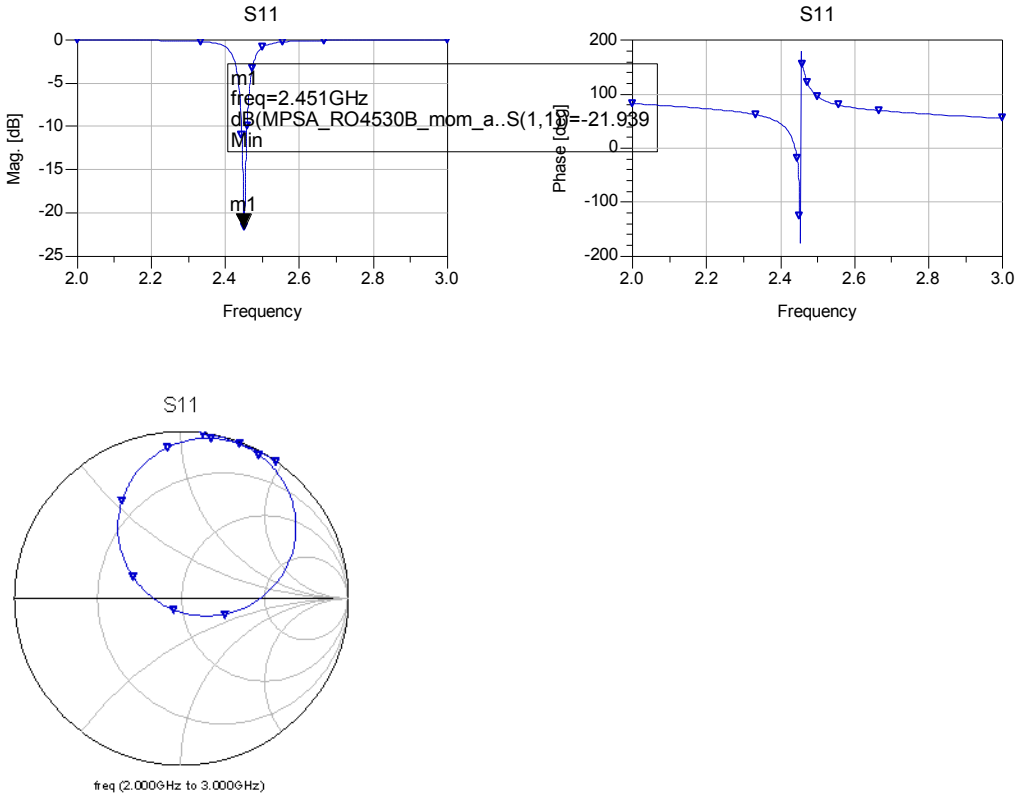

Figure 13 Antenna S-parameters

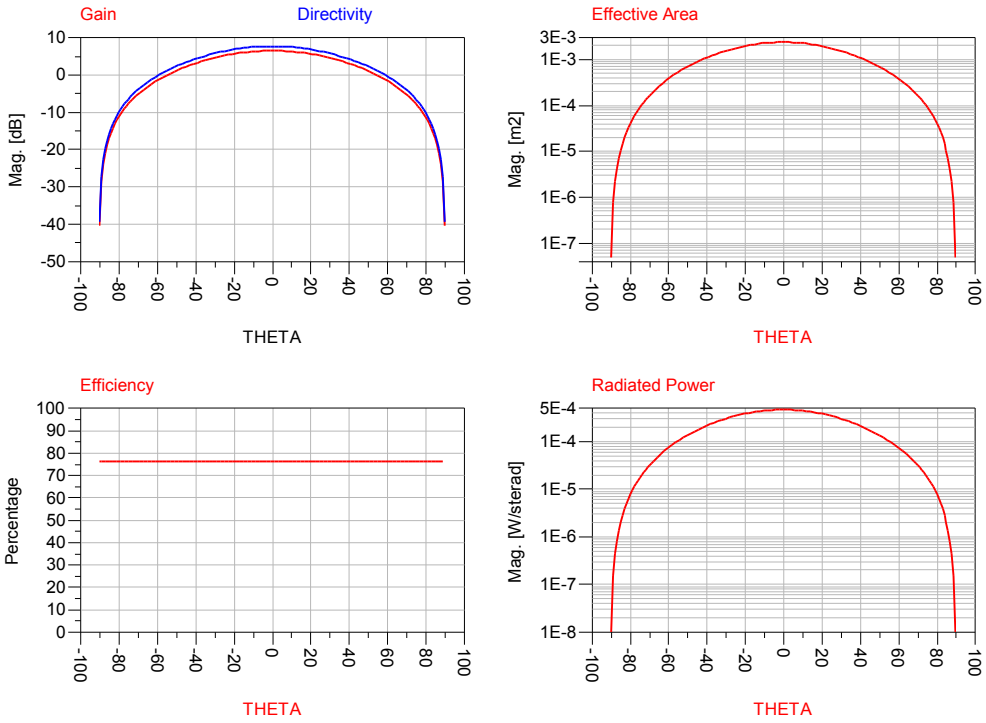

Figure 14 Patch antenna gain and efficiency

3.2 Wilkinson Power Divider

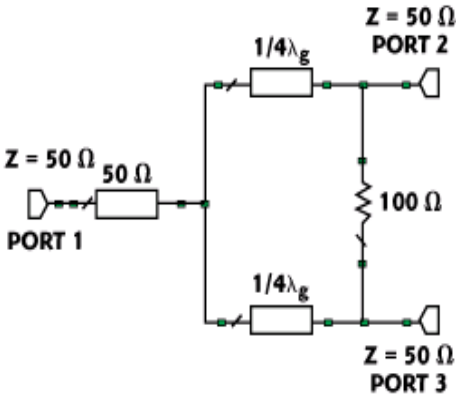

Figure 15 Traditional Wilkinson Power Divider/combiner

A four-element microstrip patch antenna with inset feed is designed to work at frequency, f = 2.45 GHz on same substrate. Element spacing is considered, $\lambda_\circ/2$ where, $\lambda_\circ$ is the free space wavelength. Any type of combiner could be used in this structure. As an example Wilkinson combiner is used to combine received RF signal on patch antennas. In general, Wilkinson power combiner has -3db insertion loss at each stage. Since we have two stages of combiner, so there are -6 dB insertion losses. This combiner provides good matching at all ports and good isolation between any couple of input ports (as combiner). When all input ports have the same input power there is no loss in this combiner. That means, signals must be coherent (same) in phase and amplitude, then no power will be dissipated. In worst case scenario, when signals are 180° out of phase, in that case the isolation resistor will dissipate a majority of RF energy. Since we have experimented a multistage rectifier, to distribute equal amount of received power in both stage of rectifiers, a Wilkinson power divider has been utilized at the output of array antennas.

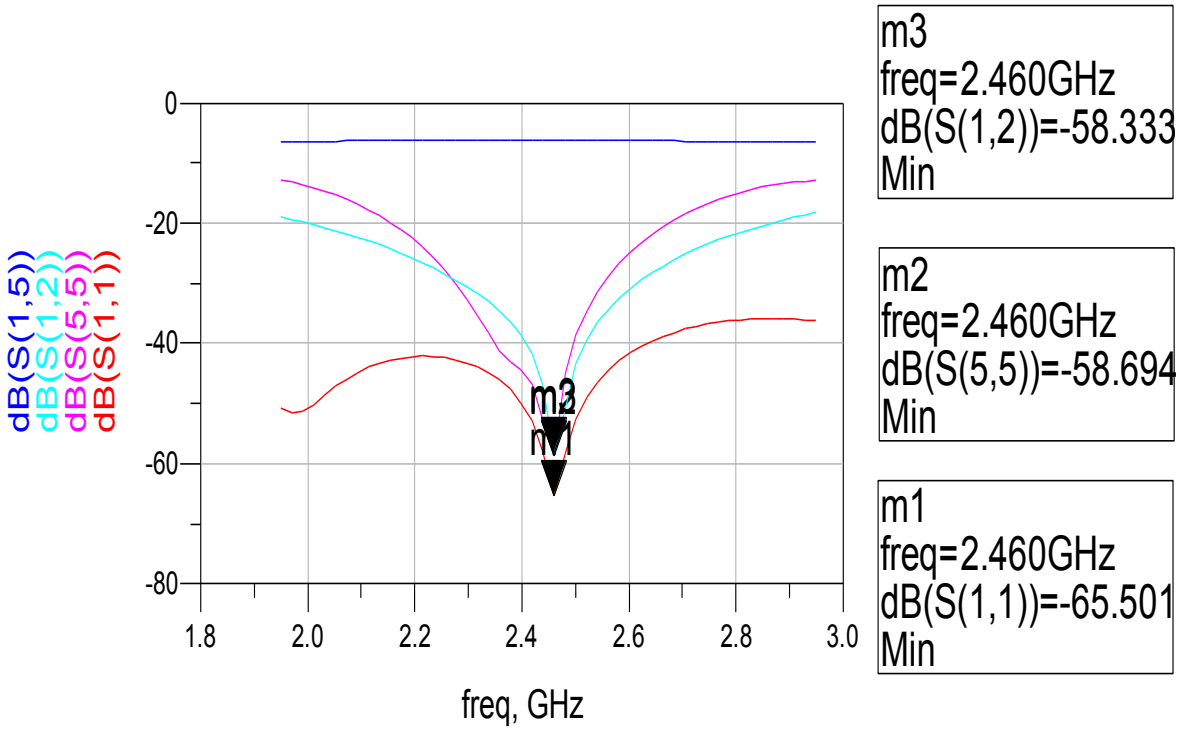

Figure 16 S-parameters of 4-way Wilkinson power splitter

3.3 Array Antenna Design

To get desired gain and to cover far field range, I have used 4 x 1 microstrip patch antenna with 6dBi gain each.

Number of Antennas	4
Element Spacing	$\lambda_o/2$

Table 2 Antenna Array Information

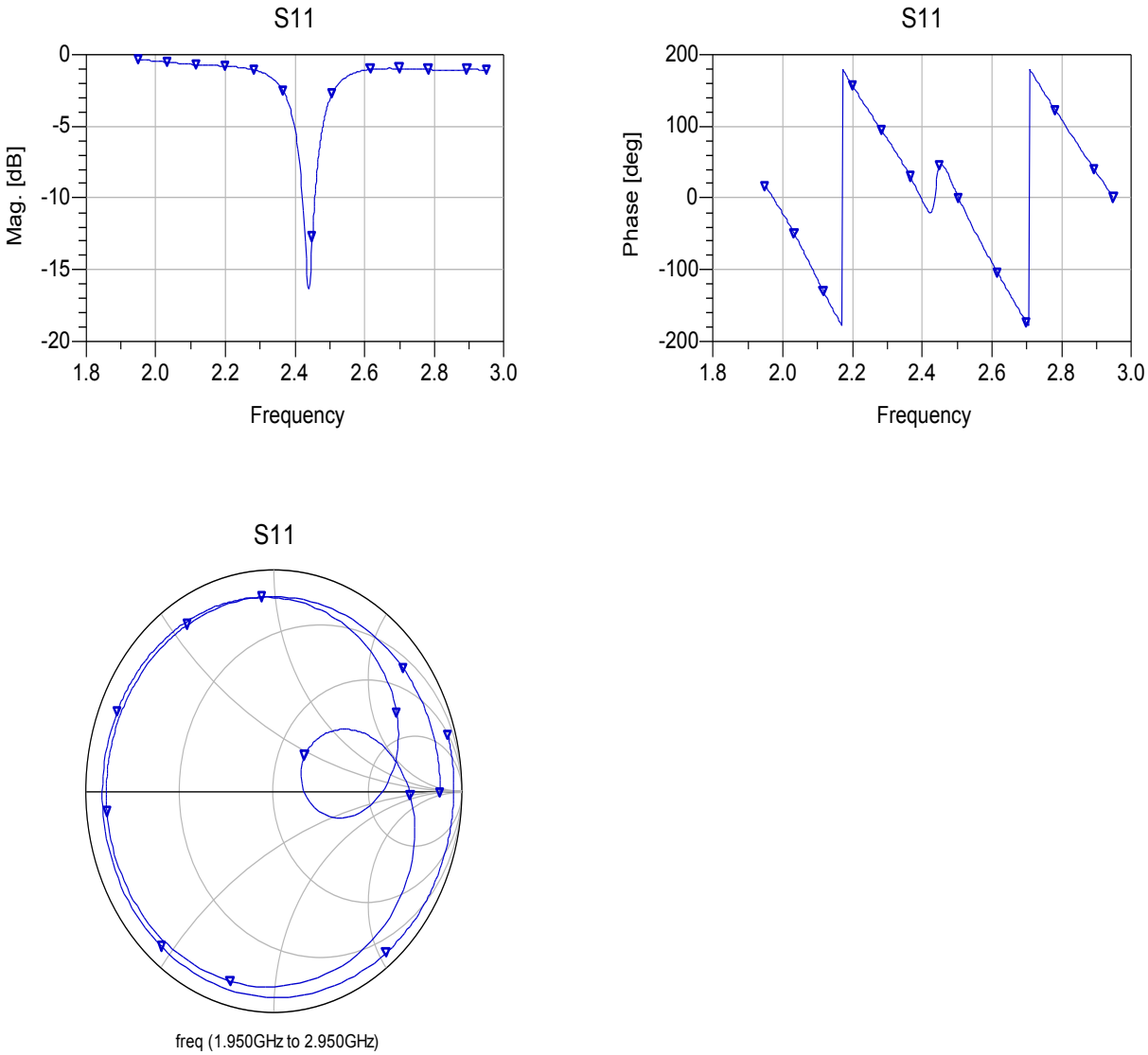

Figure 17 S-parameters for antenna array

Power

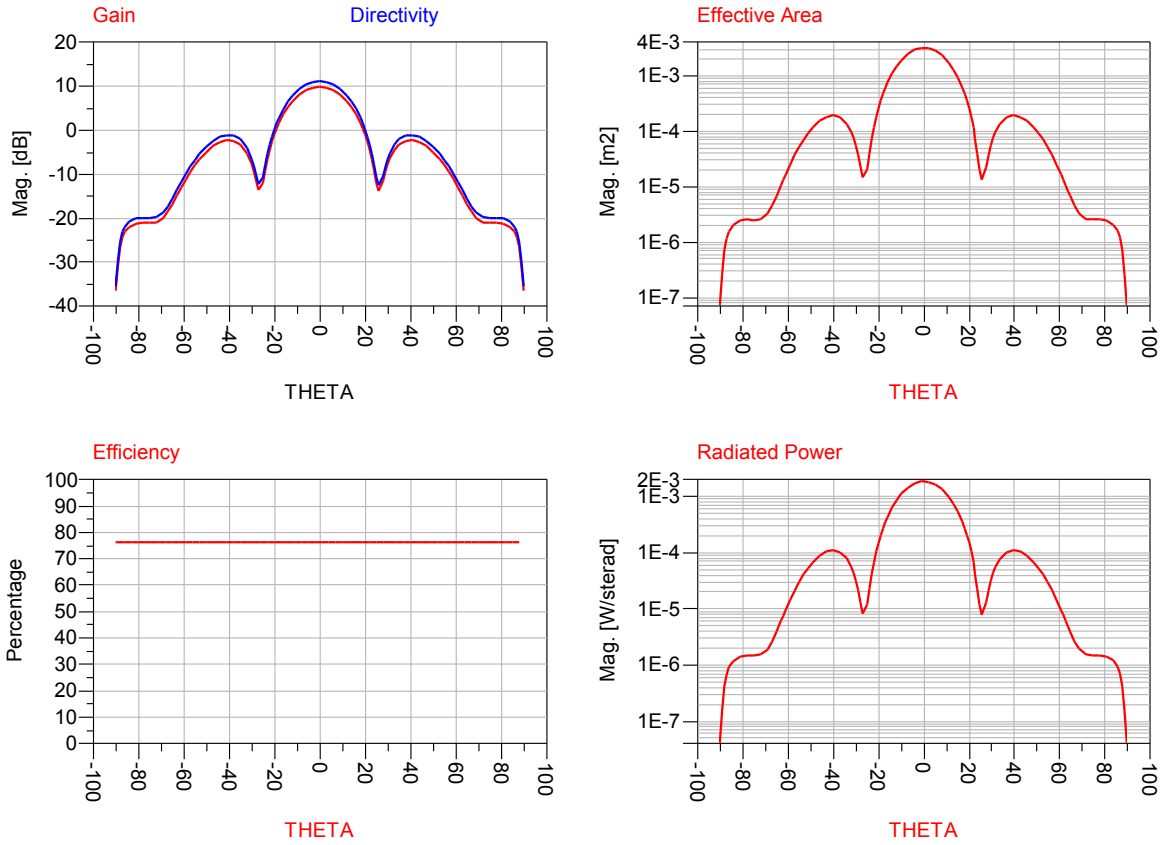

Figure 18 Gain and efficiency for array antenna

Power radiated (watts)	0.001799267475	
Effective angle (degrees)	50.33	
Directivity (dB)	11.55498329	
Gain (dB)	10.36364956	
Maximum Intensity (Watts/Steradian)	0.002048255803	
Angle of U Max (theta, phi)	18.00	90
E(theta) Max (mag, phase)	1.24228783	24.66716795
E(phi) Max (mag,phase)	0.001124618018	7.807917674
E(x) Max (mag,phase)	0.001124618018	-172.1920823
E(y) Max (mag,phase)	1.181485936	24.66716795
E(z) Max (mag,phase)	0.3838880514	-155.3328321

Figure 19 Details for antenna array parameters

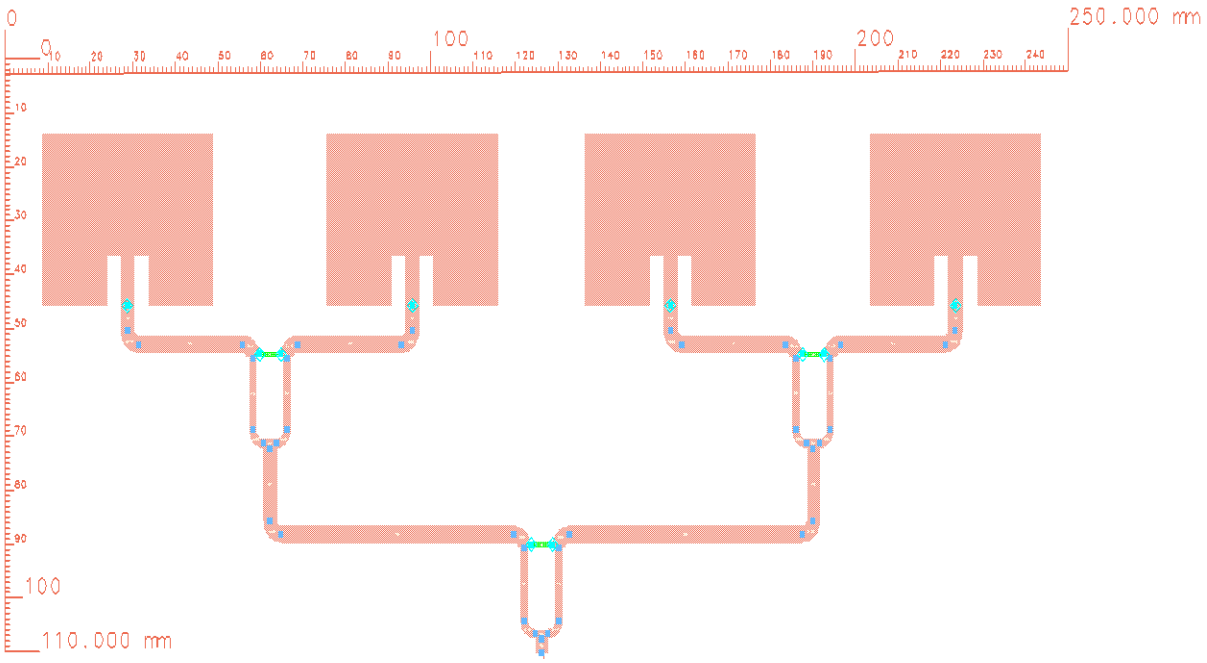

Figure 20 Four elements antenna array layout with Wilkinson power combiner

3.4 Rectifier Design

When determining the RF-to-DC conversion efficiency of rectenna, the conversion efficiency of Diode contained in rectifying circuit of rectenna is the most important parameter. For my design, two different types of zero-bias Schottky diodes have been selected to identify their rectifying efficiency. Each of these has great forward current and reverse withstand voltage among the commercial diodes

Usually, power management for energy harvesting applications requires minimum startup and supply voltage, ultra-low leakage, zero-powered standby capability and standby currents, and maximum efficiency while operating with small loads. Low-power DC-DC

converters fulfill most of these requirements and supply stable voltage and smooth current flow required for the low power application. (2)

3.4.1 Substrate Selection

An important design step is to choose a suitable substrate with appropriate dielectric constant, thickness and loss tangent. Though thicker substrates are mechanically strong, will increase radiated power, reduce conduction loss and improve bandwidth. Though, surface wave loss, dielectric loss, and extraneous radiations from the probe feed will increase. RO4350B substrate with parameters, ϵ_r=3.66, h=60 mil and tanδ= 0.034 has been chosen in this rectifier design in order to reduce noise folding. (11)

3.4.2 Diode Selection

To choose proper diodes is the first step in realizing an optimum circuit. And to do that, i have focus on voltage sensitivity of diodes and their rectifying efficiency. Based on above diode equations 1, 2 and 3; we can conclude following parameters to optimize best rectifier circuits:

1. Choice of saturation current: I_s should be lower.
2. Junction resistance, R_J is expected to be lower to receive better voltage sensitivity.
3. Low turn-on voltage another important parameter to build high efficient rectifier.

Avago HSMS-8202 and HSMS-286x Series are strong candidates for their low turn-on threshold voltage or forward voltage drop around 100 mV to ensure the diodes get turned on during each cycle. Note that added voltage source serves to oppose the flow of current until the voltage applied to the diode exceeds threshold voltage, V_{th}. In addition to the

threshold voltage drop, Schottky diodes are also preferred due to their better rectifying efficiency. These zero-bias Schottky barrier diodes are manufactured by Agilent technologies and optimized for high-frequency operation (f > 1 GHz).

Diodes SPICE parameters are summarized in following table for simulation purpose.

Parameter	Units	HSMS-286C	HSMS-8202
B_V	V	7	7.3
C_{J0}	pF	0.18	0.18
E_G	eV	0.69	0.69
I_{BV}	A	1E-5	10E-5
I_S	A	5E-8	4.6E-8
N	-	1.08	1.09
R_S	Ω	6	6
$P_B(V_J)$	V	0.65	0.5
$P_T(X_T\ I)$	-	2	N/A
M	-	0.5	0.5

Table 3 SPICE parameters for the proposed Schottky detector diodes (12) (13)

These Schottky diodes can be placed in a voltage doubler configuration. The voltage doubler produces a higher output for a given input power and offers lower input impedance to the source, simplifying the input impedance matching network. Both single and voltage doubler configuration can be realized using conventional or zero bias Schottky diodes.

In order to reduce the size of rectifier, an open circuit shunt stub could be substituted for the chip capacitor. A resistor is placed across the output terminals to act as the load for measuring the output DC power.

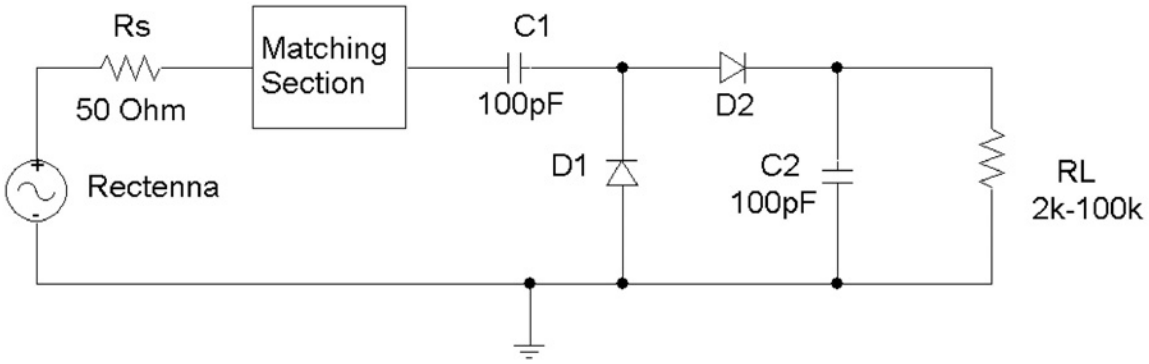

Figure 21 voltage doubler rectifier configuration (2)

Using the SPICE parameters, the first analysis of rectification properties of an HSMS8202 diode in a single detector configuration was made using Agilent Technology Design Software (ADS). For analyzing nonlinear circuits, two major techniques are recommended: the time domain based large to small signal and the frequency domain based harmonic balance analysis. Using harmonic balance simulation, resulting performance is shown in following two figures for both HSMS286C and HSMS8202 diodes.

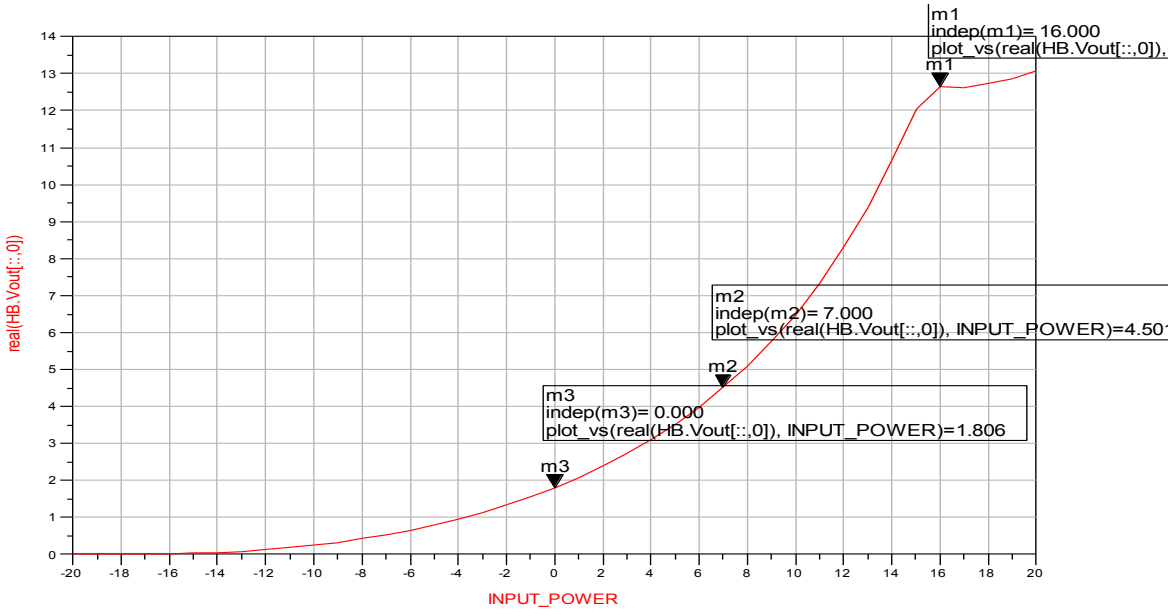

(a) HSMS8202

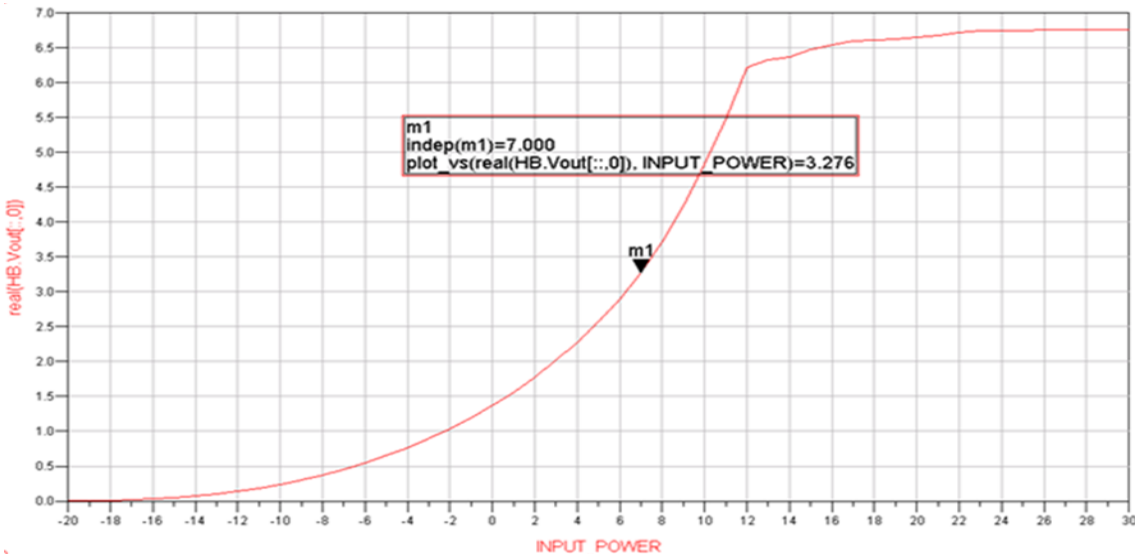

(b) HSMS286C

Figure 22 Voltage Outputs for the two proposed diodes, tuned at 7 dBm

Note that the presented voltage outputs correspond to a rectifier diode in a doubler configuration. In theory, the voltage doubler configuration doubles the output voltage compared to the single configuration at the same input power (14). The expected performances are presented in above figures accordingly. Based on these results, so far no significant difference can be seen between in either one of the diodes.

3.4.3 Diode's Impedance Matching

To reduce reflection loss as well as ensure maximum power transfer, a good impedance matching network has to be realized between the antenna and the rectifier's input. First, the diode's equivalent impedances were measured at the expected frequency range (1.95-2.95GHz) as shown below. The fundamental impedance is of importance since the front end is a tuned circuit and the "harmonic impedances" are filtered out in the application.

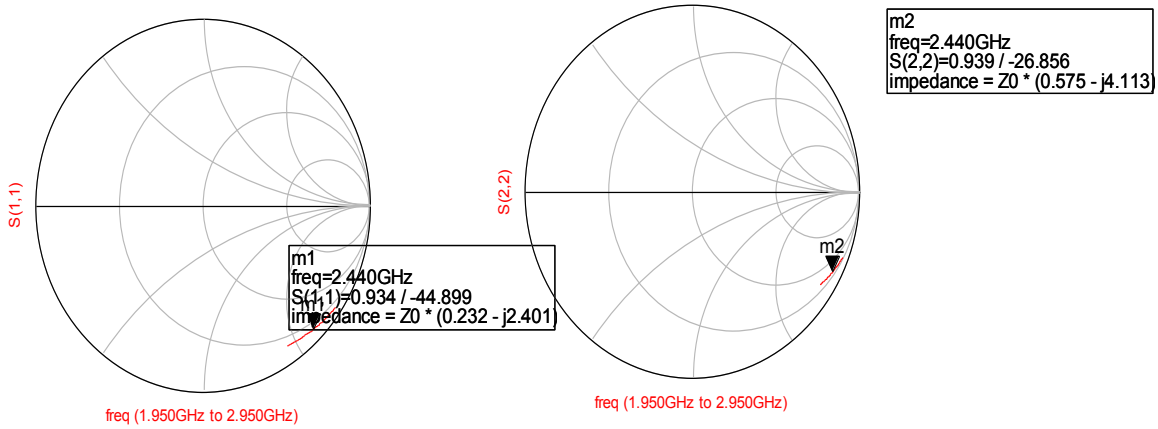

Figure 23 Double Diode's impedances

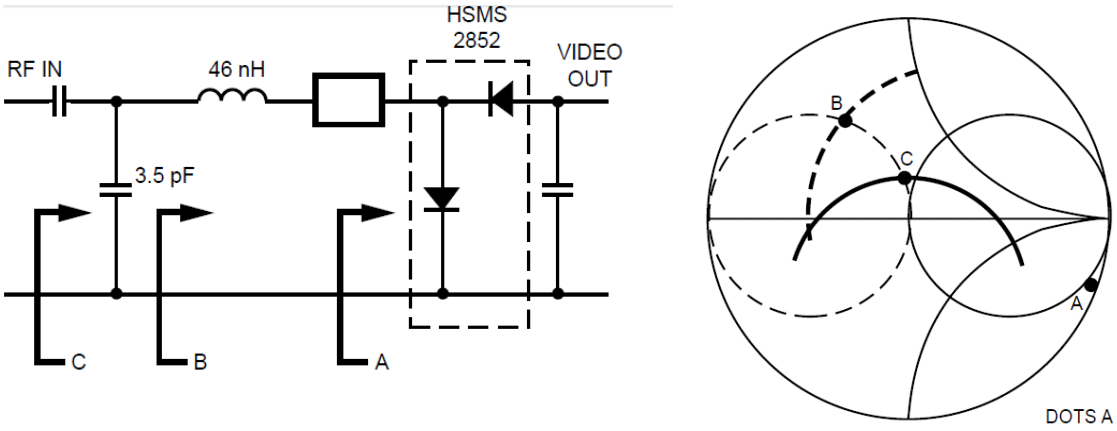

Figure 24 an example for diode's matching circuit (15)

Given the fact that diode's input impedance is little bit sensitive to the input power, the matching had to be made with a fixed input power. This design was more focused on the medium-to-low end of the input power range, which is -20dBm to 10dBm.

A single-stub matching network was designed using ADS Momentum to achieve a good impedance matching between the elements. Because of the excessive size of distributed transmission line matching elements at 2.45GHz, lumped elements were chosen for our

design. A short section of series line required to mount the diode and a series inductor rotate the impedance of the diode pair around the Smith chart to the line of constant susceptance which runs through the origin. However, a shunt inductor or shunt shorted stub cannot be used for outermost element, if we do so would short out the shunt diode, so we rotated the diode impedance up into the inductive half of the chart to the point marked B. From this point, a shunt capacitor or a shunt open circuited stub can bring the impedance down to the origin. The shunt capacitor was adjusted to keep point C just above the origin so as to obtain better bandwidth with a small sacrifice in midband match (15).

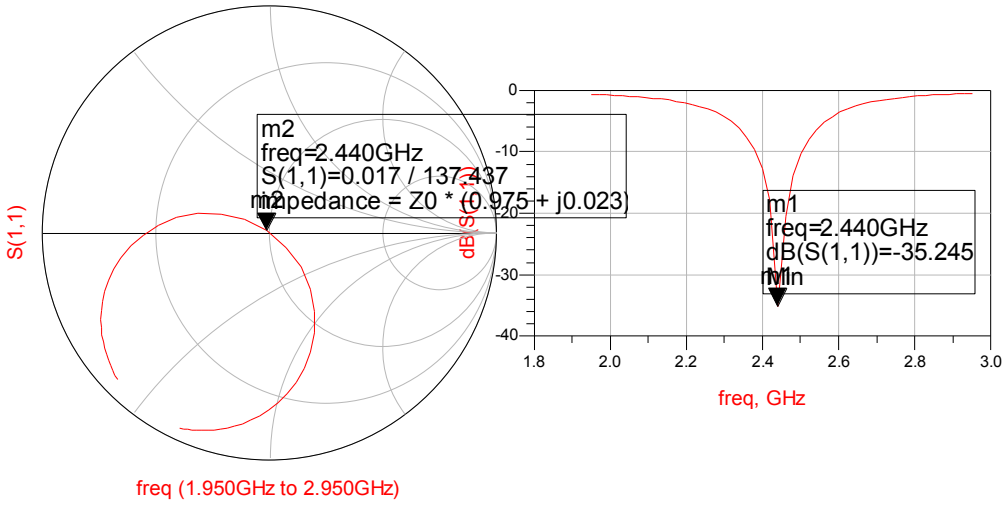

Figure 25 Design of 2.45GHz doubler matching network

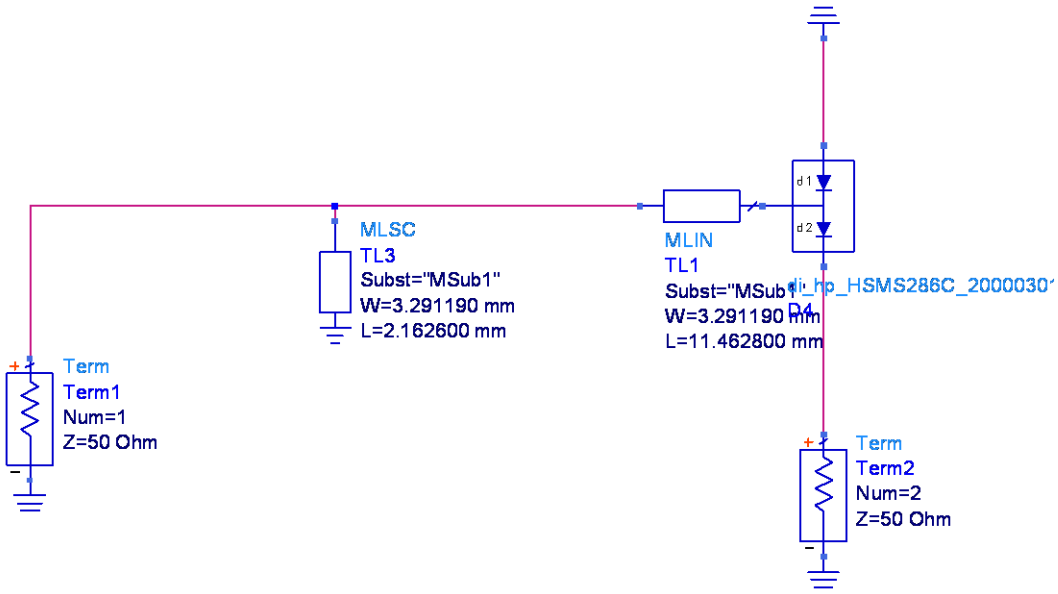

Figure 26 Matching network dimensions for HSMS286C doubler

Transfer characteristic of a Schottky diode follows a square-law rule at low power levels, with voltage output proportional to input power input. But as input power is increased, slope of the V_o/P_{in} curve flattens out to more nearly approximate a linear (voltage output proportional to RF voltage input) response. Within 20dbm, output DC voltage follows square-law with slightly masked by noise and offsets. At higher levels, the slope of the transfer characteristic depends on operating frequency, diode capacitance, and load resistance. Linear detection can be obtained by tuning or matching the diode for certain, especially high power level. Very good RF generator was used to avoid Offsets caused by meter errors. By considering of noise and offsets in my rectenna design, it was decided then to perform manual tuning with an input power of 7dBm, as was observed that as the input power increased, the performance improved than without a proper matching section. Thus, it was assumed that P_{in} = 7dBm for the proposed matching sections shown in above figure. The assumed input power corresponds to input impedances with a 13.7kΩ output load. The

Smith Chart in above shows the expected performance for the HSMS8202 matching section at 7dBm, whereas similar figure can be shown the simulated impedance match for the HSMS286C.

3.4.4 Charge Pump

A charge pump is a kind of DC to DC converter that utilizes some capacitors as energy storage elements to create either a higher or lower voltage power source. Charge pump circuits are capable of higher efficiencies, sometimes as high as 90–95% while being electrically simple circuits.

In this design, two stages charge pump using Dickson formula have been utilized , though it can be enhanced to multistage of rectifiers. Such a circuit offers several advantages:

First, voltage outputs of two diodes are added in series, which increases the overall voltage sensitivity of rectifier circuits, compared to a single diode detector.

Second, reactive matching for rectifier circuits becomes much easier when RF impedances of the two diodes are added in parallel.

But while designing this charge pump circuit we have to be careful about diode's threshold voltage, threshold voltage drops at multistage rectifier will completely kill the input voltage leaving no voltage on the output.

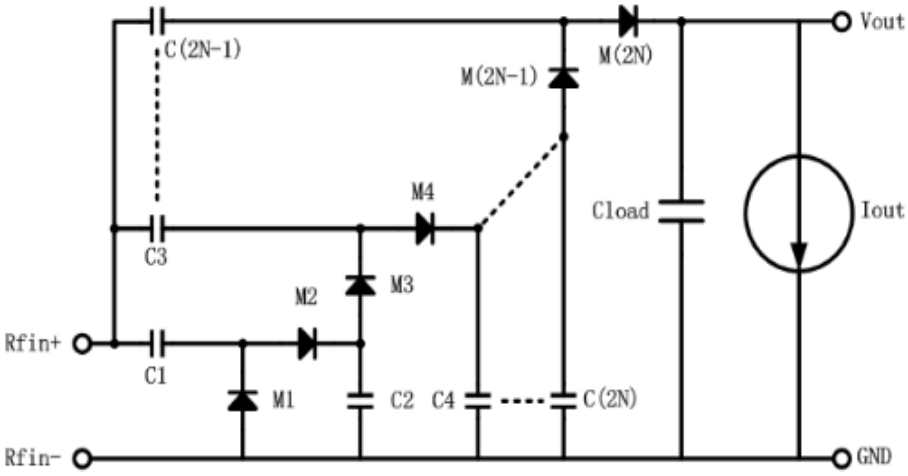

Figure 27 N-stage Charge Pump

DC to DC converters are widely used in different applications and purposes. The buck, boost, buck-boost, and C´uk converters can have realistic power efficiencies around 90%. Using inductor and large capacitors, the Cockcroft-Walton voltage multiplier can have power efficiency very close to 1.0 if operating at very high voltage. However, it has some problem when stray capacitance becomes comparable to capacitors shown in the figure.

Among these, Dickson charge pump overcomes many of the shortcomings of these converters. First, inductors were not used here. Second, it suffers only half as much from stray capacitance as does the Cockcroft-Walton voltage multiplier (4). One disadvantage is its nonlinear gain, in order to control the output a more complex feedback system needs to be designed.

3.4.5 Wilkinson Power Divider

In order to distribute equal amount of receiving power in both stage of rectifiers, a Wilkinson power divider has been attached at input level. To do that, we had to confirm,

incoming signals must be coherent (same) in phase and amplitude. When they are in phase and amplitude, the voltage potential at each end of the rectifier will be same so no power will be dissipated. Using the reverse method of Wilkinson power combiner in antenna section, this divider was constructed with isolation and return loss described there.

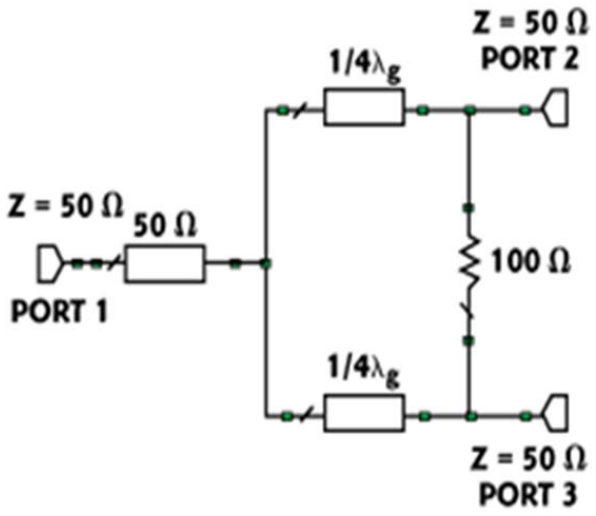

Figure 28 Wilkinson power divider configuration

3.4.6 Fabricated Rectifiers

Physical realization of one of the rectifiers is shown in the following figure. After performing all kinds of necessary simulation, Gerber files were generated for fabrication purpose using ADS. After that i contacted with local microwave circuit manufacturing company for fabrication and at the end, I was able to create two rectifiers circuits for further analysis.

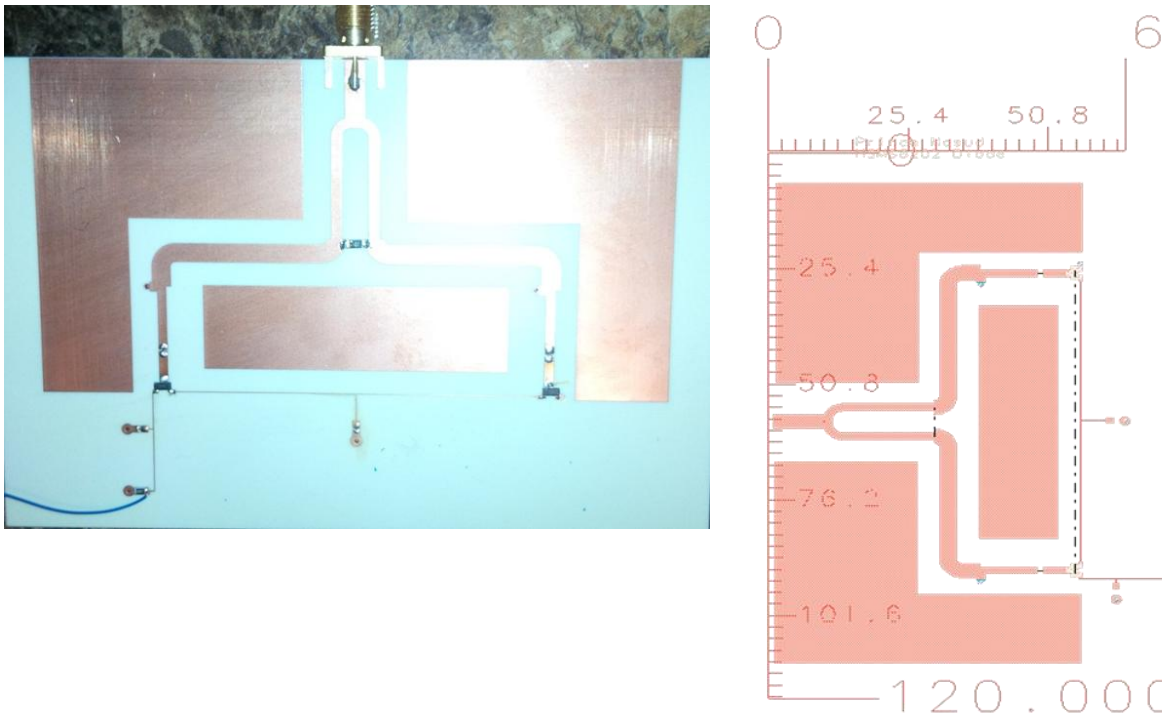

Figure 29 Fabricated Rectifier and its ADS layout

3.4.7 Efficiency Calculation

In testing rectenna in a waveguide simulator, an overall efficiency (η_O) and rectifier conversion efficiency (η_C) *are* defined as below:

$$\eta_O = \frac{dc\ output\ power}{incident\ RF\ power}$$

$$\eta_C = \frac{dc\ output\ power}{incident\ RF\ power - reflected\ RF\ power} = \frac{P_{dc}}{P_r} = \frac{V_o^2}{R_L P_r}$$

where P_{dc} is the DC output power, P_r is the received RF power into rectifier circuit, and V_o is the DC output voltage detected at the load resistor. The performance of the rectifier circuit is measured by performing non-radioactive method where the total rectenna

conversion efficiency is measured in available radioactive method using an omnidirectional transmit antenna of gain, G_t=2.2 dBi and with different transmit power range and the load resistance, R_L=7.87Kohm for HSMS-286C and 13.7K ohm for HSMS-8202 diodes around 2.45 GHz.

3.4.8 DC pass/output filter Design

This output filter consisting of a large capacitor effectively shorts the Microwave energy and passes the DC power. The distance between the diode and output capacitor is used to resonate the capacitive reactance of the diode. Both input and output capacitors are used to store microwave energy during the off period of the diode.

Finally, the capacitor separates the RF from the video sides of the circuit. It must provide a good RF short circuit to the diode, to insure that all of the RF voltage appears across the diode terminals. However, it must be small at video frequencies, so that it does not load down the video circuit.

3.4.9 Output load

The output load resistance of the rectifying circuit R_L is varied to obtain the desired $I_{out.}$ After receiving maximum rectification efficiency out of this rectifier circuit, we can change the output load to obtain desired I_{out}. Rectification efficiency of the two rectifier circuits was measured at an incident power level of +7 dBm as a function of load resistance; data is presented in above tables. It illustrates that parasitic series resistance can have the significant effect on the efficiency of the rectifier circuit. Peak efficiency was achieved at a load resistance of approximately 2KΩ, a practical value for rectenna applications.

Chapter 4: Experimental Results

4.1 Measured Antenna Performance

The fabricated antenna is shown in following figure. Actual lab measurement of the antenna's radiation pattern was made in RIM's RF anechoic chamber; Both VSWR and Input Impedance were obtained using an Agilent Technologies 8714C Network Analyzer. The measurement of these data can provide useful information about the expected antenna's performance.

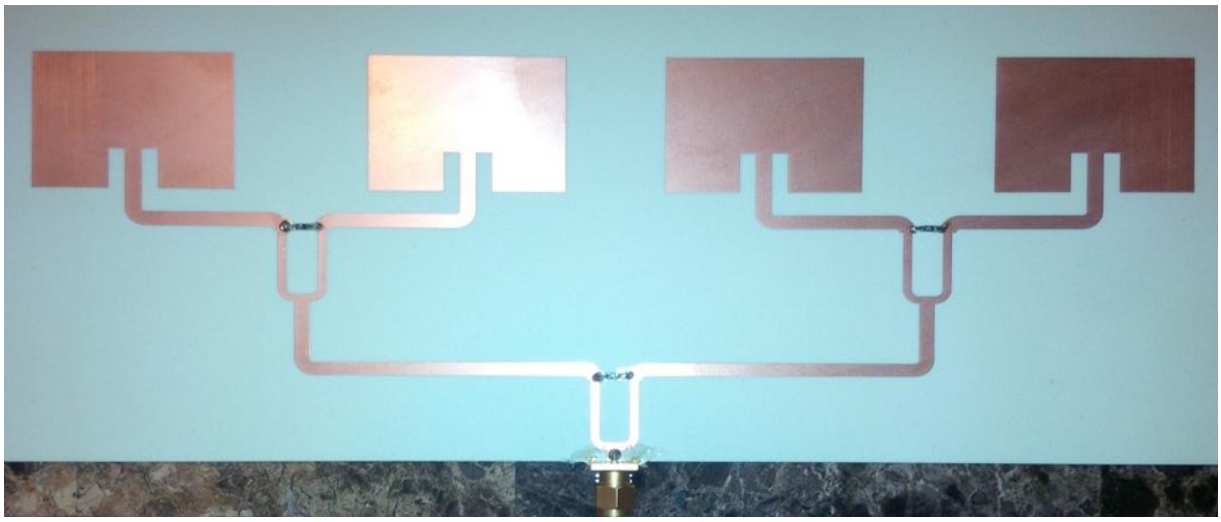

Figure 30 Fabricated Final Antenna

Figure 31 shows measured Input Return Loss, VSWR and complex Input Impedance of the antenna that was analyzed as discussed previously. It can be observed that the center frequency of microstrip array antenna is located at 2.45GHz with an input return loss close to -7dB, and an approximate bandwidth of 30MHz. This return loss will have to improve in my future design. The input impedance at the center frequency was measured to be very close to the desired 50Ω value.

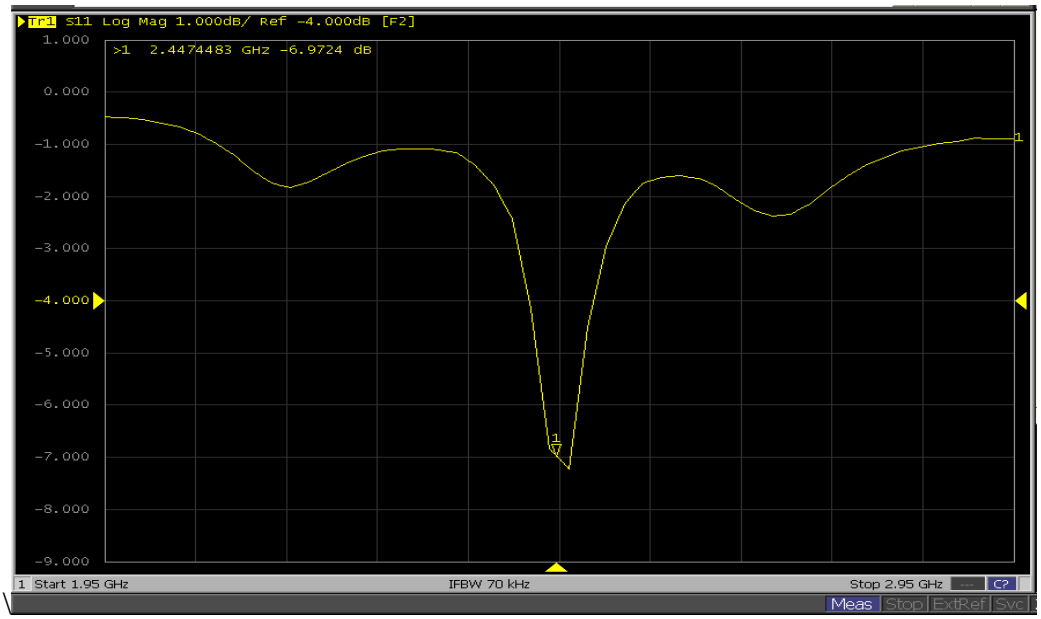

Figure 31 Antenna Return Loss

Later this fabricated antenna was taken into RIM's Anechoic Chamber for further analysis. Using "radiated power passive antenna" testing method, antenna radiation pattern was measured for different frequencies as shown in following table. Though expected gain was around 11 dB, but during antenna fabrication, metal ground plane was not placed back of antenna by mistake. So, as an alternative, copper tape was attached on the back of this antenna which reduces actual gain of this antenna to 8.1 dB.

Frequency (MHz)	2440	2450
Ant. Port Input Pwr. (dBm)	0	0
Tot. Rad. Pwr. (dBm)	-1.6358	-1.3444
Peak EIRP (dBm)	8.1099	8.1291
Directivity (dBi)	9.7456	9.4735
Efficiency (dB)	-1.6358	-1.3444
Efficiency (%)	68.6158	73.3767
Gain (dBi)	8.1099	8.1291
NHPRP +/-Pi/4 (dBm)	-5.1216	-4.6253
NHPRP +/-Pi/6 (dBm)	-7.2805	-6.7668
NHPRP +/-Pi/8 (dBm)	-8.6598	-8.1421
Upper Hem. RP (dBm)	-2.2683	-1.9899
Lower Hem. RP (dBm)	-10.315	-9.9423
NHPRP4 / TRP Ratio (dB)	-3.4858	-3.2809
NHPRP4 / TRP Ratio (%)	44.8143	46.9802
NHPRP6 / TRP Ratio (dB)	-5.6447	-5.4224
NHPRP6 / TRP Ratio (%)	27.2603	28.6918
NHPRP8 / TRP Ratio (dB)	-7.024	-6.7976
NHPRP8 / TRP Ratio (%)	19.8424	20.9043
UHRP / TRP Ratio (dB)	-0.6326	-0.6455
UHRP / TRP Ratio (%)	86.4456	86.1894
LHRP / TRP Ratio (dB)	-8.6792	-8.5979
LHRP / TRP Ratio (%)	13.5544	13.8106
Front/Back Ratio (dB)	13.0357	13.4065
Phi BW (deg)	345.8	325.8
+ Phi BW (deg)	263.9	254.1
- Phi BW (deg)	81.9	71.7
Theta BW (deg)	136.5	144.2
+ Th. BW (deg)	60.8	63.3
- Th. BW (deg)	75.7	80.9

Table 4 Measured actual antenna parameters

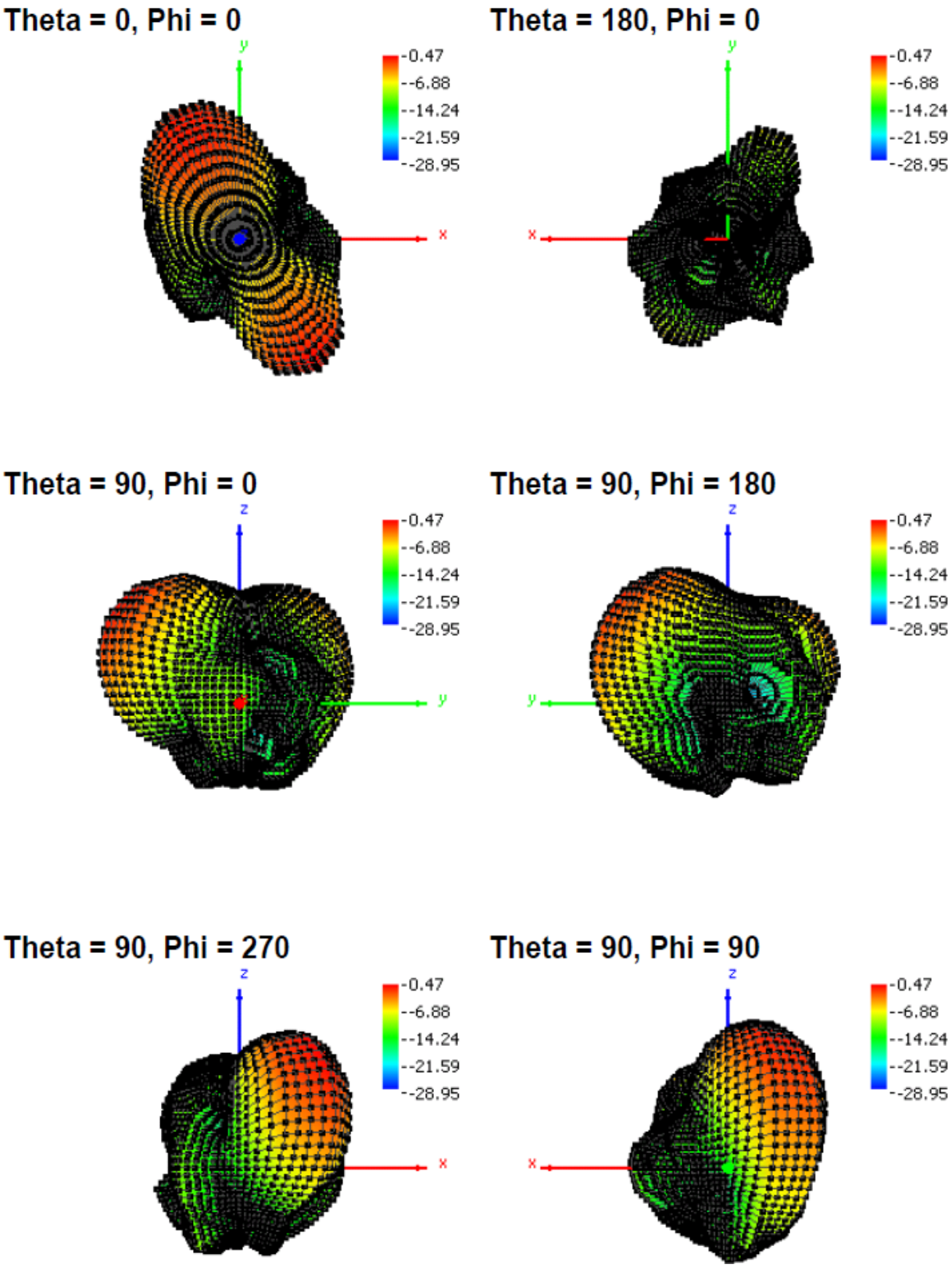

Figure 32 Measured values for the designed inset-fed patch array antenna

4.2 Measured Rectification Data

Using network analyzer, maximum return loss was first measured for the rectification circuits. Given the fact that the input impedance of the diodes is sensitive to the input power, we have realized that maximum rectification efficiency was achieved at f= 2.232GHz for HSMS-8202 and f= 2.246GHz for HSMS-286C diodes. But as per our design, maximum rectification efficiency was expected around 2.45 GHz. This frequency mismatch could be happened during fabrication, due to slide change of substrate parameters. Measurement results are shown for both rectified diodes-HSMS286C and HSMS8202 in following table 4 and 5.

Table 4 shows the obtained voltages using the HSMS8202. The rectification efficiency is higher around the end power levels, which is expected due to the fact that the matching section is optimized at those levels. The efficiency values range from 50% in the lower power end and up to 70% near the medium-to-high power levels. It is important to notice that the other diode pair, the HSMS286C, has almost similar performance for the same levels. From this table, it can be observed that HSMS8202 has better conversion efficiency at low power level whereas HSMS286C is good at high input power.

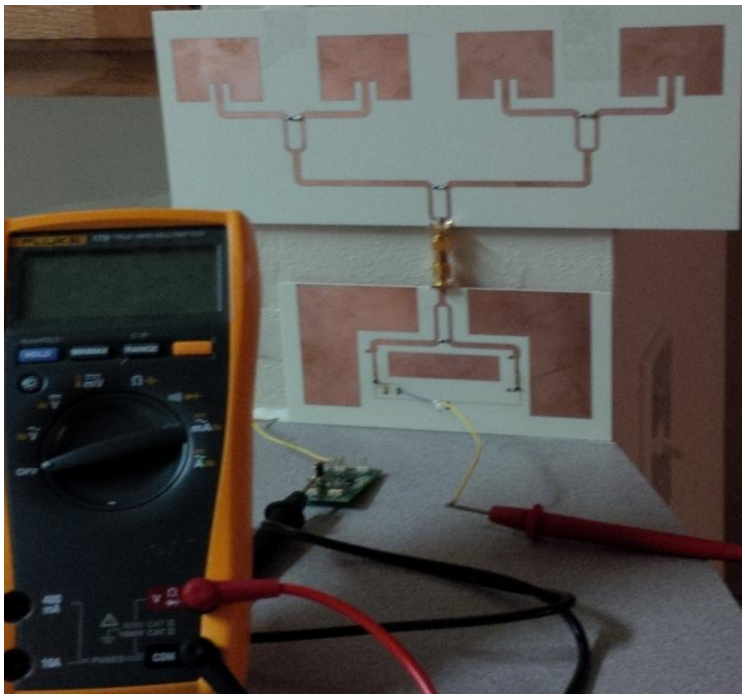

Figure 33 Complete rectenna circuit using HSMS8202

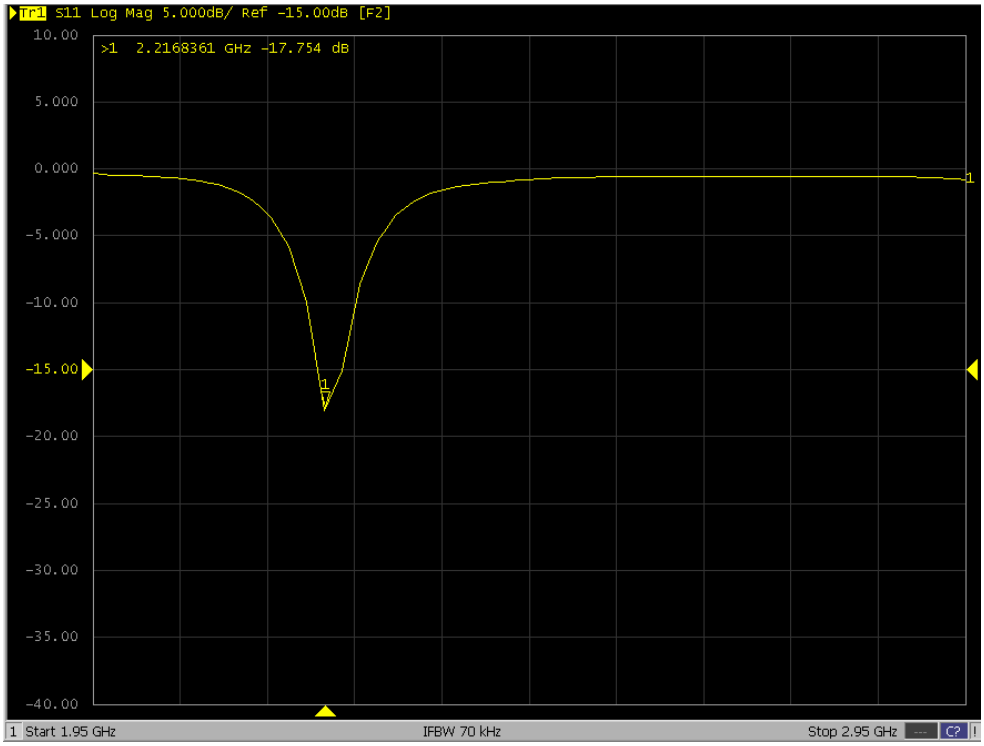

Figure 34 Measured Input Return Loss for HSMS8202 Matching Circuit, R_L = 13.7kΩ

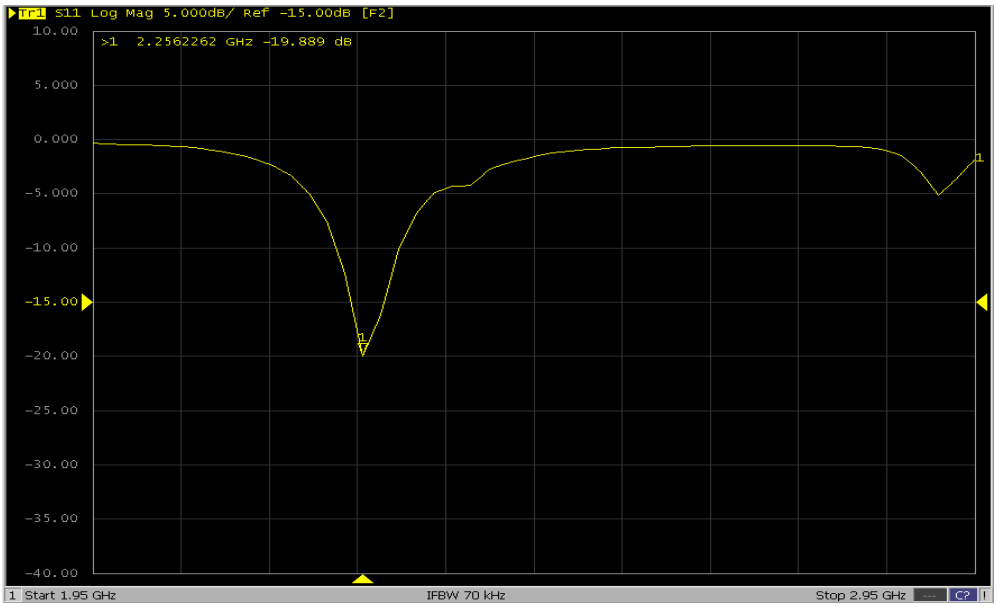

Figure 35 Measured Input Return Loss for HSMS286C Matching Circuit, R_L = 7.87kΩ

P_{in}[dBm]	P'_{in}[dBm]	P'_{in}[mW]	V_{out} [V] at f=2.232GHz R_L = 13.7KΩ	P_{out}[mW]	Efficiency[%]
-10	-10.6	0.087096359	0.32	0.007474453	8.58
-9	-9.6	0.10964782	0.412	0.012390073	11.30
-8	-8.6	0.138038426	0.52	0.019737226	14.30
-7	-7.65	0.171790839	0.643	0.030178759	17.58
-6	-6.65	0.216271852	0.783	0.044751022	20.69
-5	-5.67	0.271019163	0.94	0.06449635	23.80
-4	-4.67	0.341192912	1.118	0.091235328	26.74
-3	-3.67	0.429536427	1.318	0.126797372	29.52
-2	-2.67	0.540754323	1.557	0.176952482	32.72
-1	-1.67	0.680769359	1.815	0.24045438	35.32
0	-0.65	0.860993752	2.103	0.322818175	37.49
1	0.25	1.059253725	2.432	0.43172438	40.76
2	1.23	1.327394458	2.796	0.570628905	42.99
3	2.25	1.678804018	3.212	0.753061606	44.86
4	3.21	2.094112456	3.674	0.98527562	47.05
5	4.26	2.666858665	4.194	1.283915036	48.14
6	5.2	3.311311215	4.77	1.66079562	50.16
7	6.19	4.159106105	5.442	2.161705401	51.98
8	7.19	5.236004366	6.185	2.792279197	53.33
9	8.19	6.591738952	7.02	3.597109489	54.57

10	9.26	8.433347578	7.99	4.659861314	55.26
11	10.22	10.51961874	9.15	6.111131387	58.09

Table 5 Measured Voltages for the HSMS-8202 rectification circuit

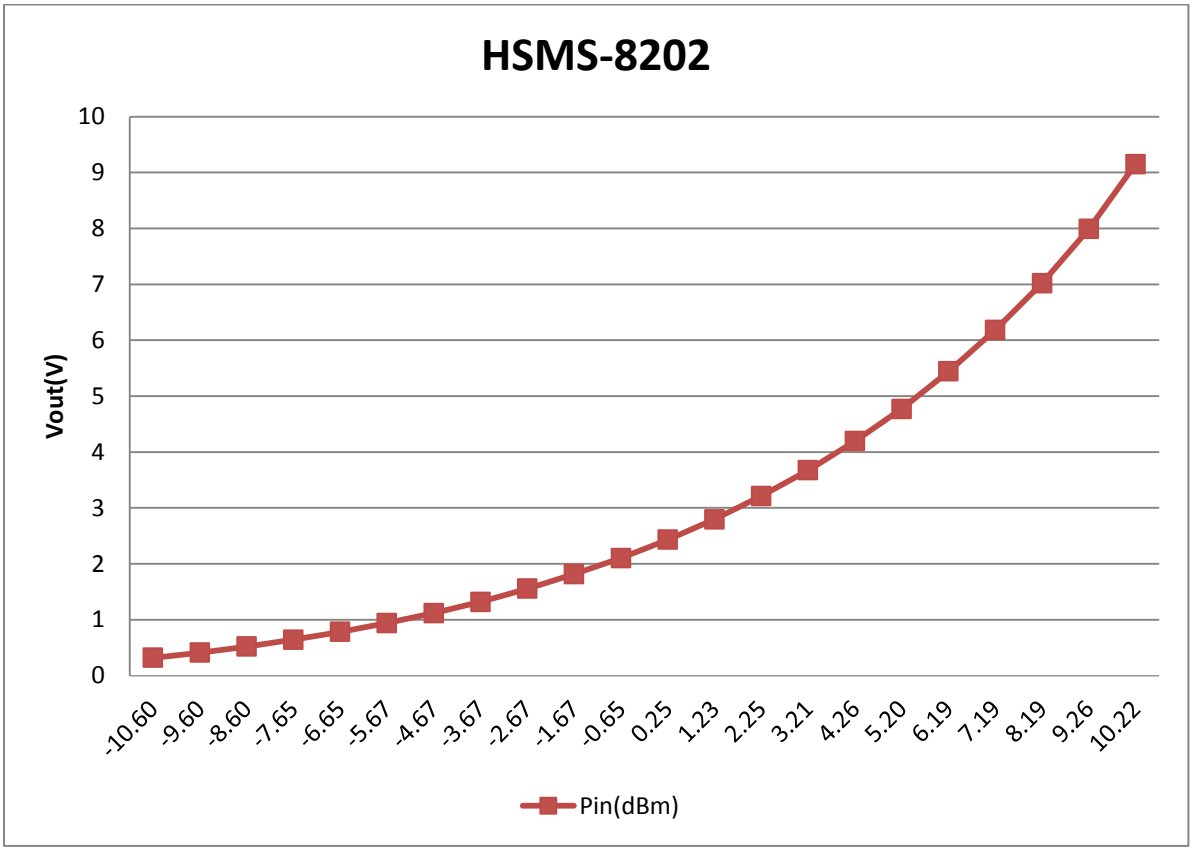

Figure 36 Graphical representation of measured voltages for the HSMS-8202 rectifier

P_{in}[dBm	P'_{in}[dBm]	P'_{in}[mW]	V_{out} [V] at f=2.246GHz $R_L = 7.87K\Omega$	P_{out}[mW]	Efficiency[%]
-12	-12.6	0.054954087	0.123	0.001922363	3.50
-11	-11.6	0.069183097	0.172	0.003759085	5.43
-10	-10.6	0.087096359	0.231	0.006780305	7.78
-9	-9.68	0.107646521	0.301	0.011512198	10.69
-8	-8.68	0.135518941	0.384	0.018736468	13.83
-7	-7.68	0.170608239	0.482	0.029520203	17.30
-6	-6.68	0.214783047	0.591	0.044381321	20.66
-5	-5.68	0.270395836	0.715	0.064958704	24.02
-4	-4.68	0.34040819	0.855	0.092887548	27.29
-3	-3.68	0.42854852	1.013	0.130389962	30.43

-2	-2.68	0.539510623	1.198	0.182363914	33.80
-1	-1.68	0.679203633	1.406	0.251186277	36.98
0	-0.68	0.855066713	1.635	0.339672808	39.72
1	0.21	1.049542429	1.893	0.455330241	43.38
2	1.23	1.327394458	2.187	0.607747014	45.79
3	2.2	1.659586907	2.524	0.809475985	48.78
4	3.2	2.089296131	2.897	1.06640521	51.04
5	4.18	2.618183008	3.316	1.397186277	53.37
6	5.18	3.296097122	3.79	1.825171537	55.37
7	6.17	4.139996748	4.33	2.382325286	57.54
8	7.18	5.22396189	4.939	3.099583355	59.33
9	8.18	6.576578374	5.624	4.018980432	61.11
10	9.24	8.394599865	6.42	5.237153748	62.39
11	10.22	10.51961874	7.39	6.939275731	65.97

Table 6 Measured voltages for the HSMS-286C rectification circuit

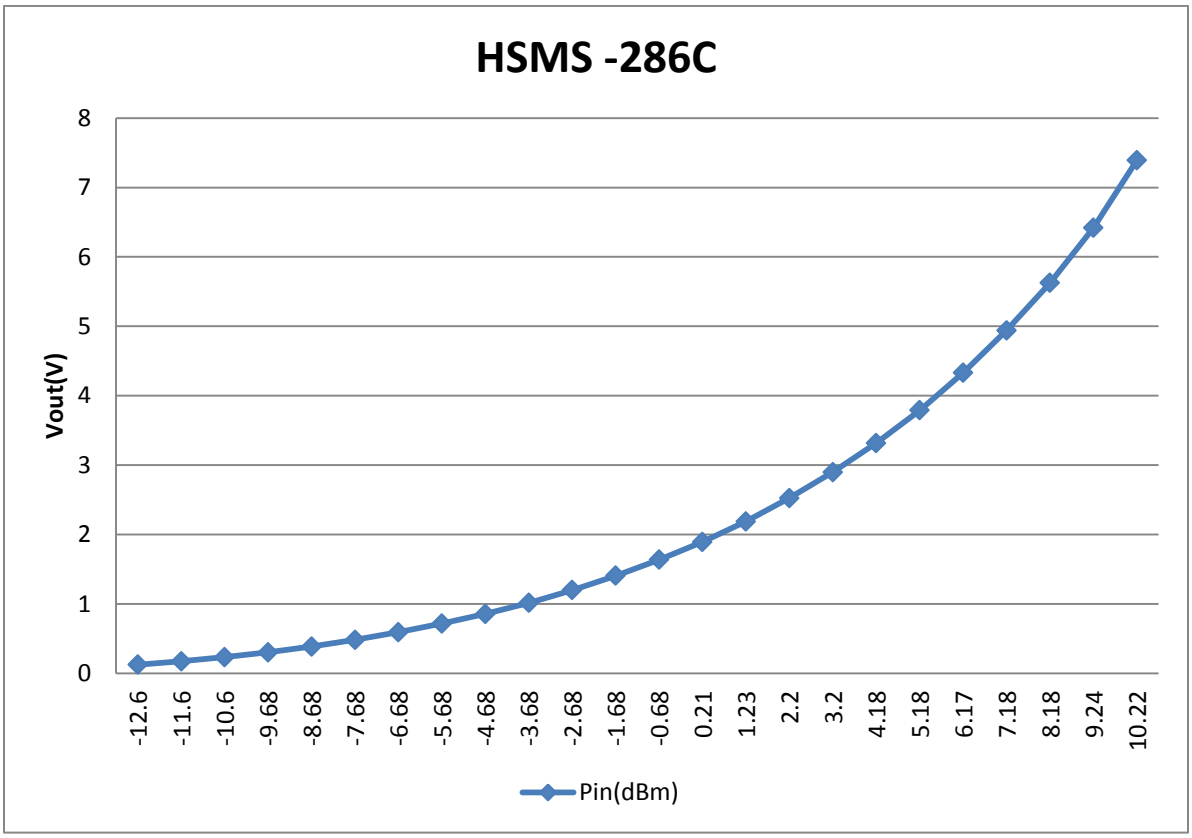

Figure 37 Graphical representation of measured voltages for the HSMS-286C rectifier

4.3 Measured Link Data

In order to transfer power efficiently, a horn antenna with high directivity broad bandwidth should be used as the transmit antenna power generated by the signal generator and then delivered to the antenna.

The laboratory setup that commonly used to characterize the Radio Link is shown in following figure. The amount of transmitted power was also restricted by the laboratory equipment, where the HP Signal generator could able to produce transmitted power up to 20dBm. According to FCC regulations, the maximum transmitted power should not more than 1W.

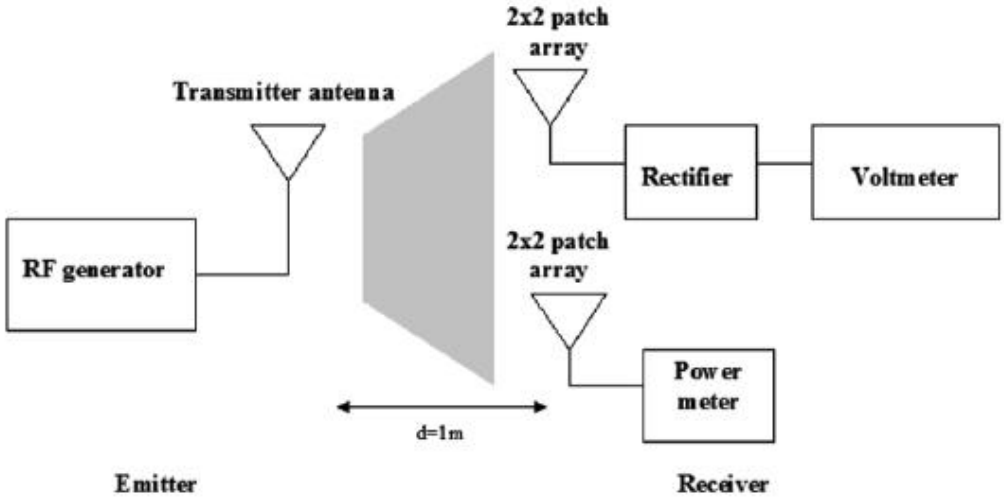

Figure 38 Block Diagram for Power Link Test (16)

Since our primary objective was to utilize the power transmission from WLAN or cellular network, but the received power at rectenna end becomes significantly low over distances. Using friis equation discussed above, I have tried to model this mathematical equation for maximum transmit power, P_t = 20dBm, transmitter antenna gain = 2.2dB,

receiver antenna gain = 8dB and frequency = 2.45 GHz. Finally I derived following radio link performance model. It shows that received power significantly decreases over distances for the current scenario. Though if we could use a high gain transmitting horn antenna with maximum allowable transmitted power, then received power at rectenna end will be improved over distances.

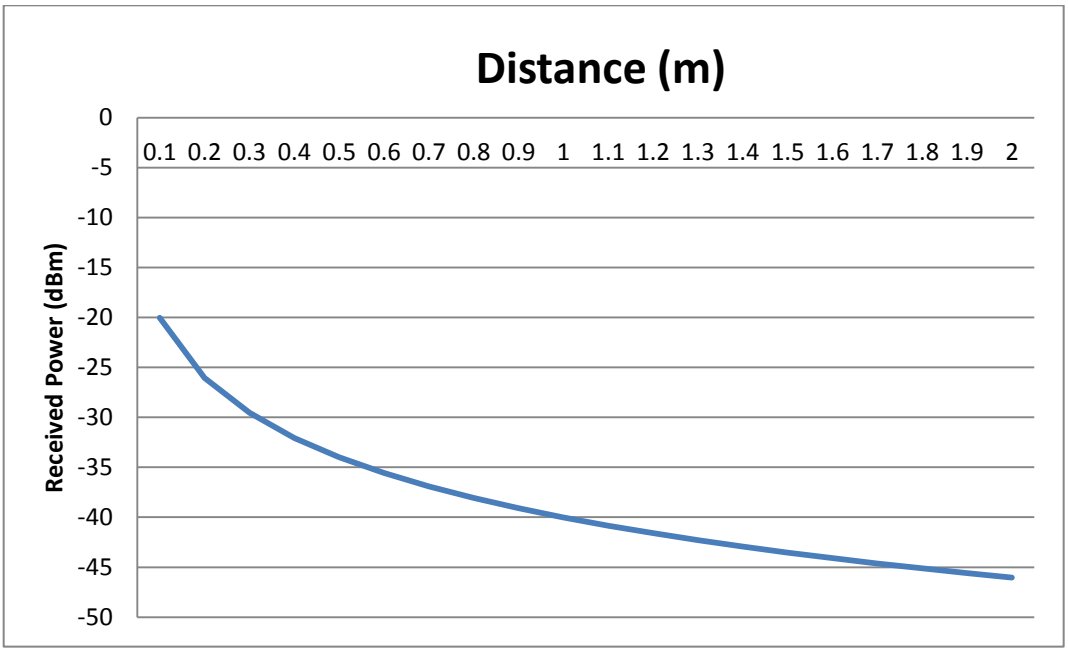

Table 7 Radio link performance for P_t=20dBm, G_t=2.2dB, G_r=8dB and freq=2.45GHz

For this current scenario and using radioactive method, I was finally able to measure overall rectenna performance using for two fixed distances which was summarized in following table.

Distance [cm]	Measured Power [V]
10	0.4
20	0.325

Table 8 Measured power for the experimental Radio Link

Though this radio link performance is poor compared to that expected from the

theory obtained during link budget calculation. This can be due to several reasons. Attenuation effects are discarded because the laboratory environment is somewhat free of humidity and particles. Since this designed rectifier's operating frequency has changed from 2.45GHz to around 2.2GHz, this change has significant effect on overall rectenna performance. During lab test, omnidirectional transmitting antenna was used instead of recommended horn antenna. Another important consideration is the unexpected attenuation of the transmitting cable. Also, the radiation patterns of the antennas are broad, and multipath effects could exist that create destructive interference of the signals arriving at the antenna on the receiver's side. For future improvements, a more complete radio link model analysis should be made, where phase delays, rectifier fabrication and multipath will be taken into consideration.

Chapter 5: Conclusion

A 2.45 GHz rectenna system has been analyzed, discussed, designed, and tested in the present dissertation, to explore the idea of getting rid of cables as well as batteries while in cellular or Wi-Fi coverage.

First, a microstrip patch antenna with compact size was designed, simulated and implemented. The theoretical design procedure was straightforward; the simulations obtained from this design shown very acceptable performances in the frequency band of interest. In next implementation level, a microstrip array antenna was implemented to obtain the desired gain at desired frequency of 2.45GHz. Using simple and manual tuning method, a direct control of the antenna's resonant frequency was obtained.

Using the proper equipment and facilities at Research in Motion, the radiation properties of the antenna has been measured. This design and testing relied entirely on other properties of the antenna such as Voltage Standing Wave Ratio (VSWR) and Input Impedance. The resulting measurements of these properties were satisfactory. It was observed that RO4350B material selected as the dielectric of the antenna had good radiation performance, though RT/duroid 5880 substrate could be used as an alternative and for better performance. Little or no attention was paid to the associated ground plane of the antenna. Increasing its size will definitely improve the antenna efficiency as well as can provide higher gains in the direction of interest. Nonetheless, a more directive antenna with a narrower beam could be used to concentrate more energy within a small area, thus having a highly power dense rectenna can convert to usable DC power.

A rectifier was also analyzed, designed, and implemented using Dickson charge pump method. Using two different types of diode pairs, it was observed that both diodes presented very similar rectification properties from both theoretical and practical point of view. In the impedance matching section, the stub lengths were acceptable for both diodes and the match was achieved with very good results. The impedance match of both diodes was key when measuring their rectification properties. HSMS-286C provided higher efficiencies, above 65% as stated in table 5 for low input power 10dBm. Though for similar input power range, HSMS-8202 provides 58% efficiency.

Finally, the complete rectenna system was used to measure overall performance on WLAN test environment, which was the primary objective of this design. The maximum distances obtained in lab tests ($\leq$ 2m), certainly were less than theoretical values. Since basic link model that was used, multipath effects and fading due to elements in the line-of-sight were not taken into account. More complex model that considers all these effects can be realized and used to predict the real performance of rectenna system in WLAN or Cellular environment.

5.1 Future Work

Every day technology is being improved, also by virtue of nano-technology; new diodes and sensor technologies are coming in the market. Thinking about the possible future of a wireless power receiver system like the one presented in this dissertation, the possibilities appear attractive when focused on new low threshold voltage diodes. First, one could think of a world where low power batteries, like the coin-cell type ones, have evolved in a way such that there is no need to replace them. They could become permanent recharging batteries thanks to an existing wireless power source in our surroundings.

As for future research in charge pump based rectenna system, more complicated arrays could be used. For example, a eight element array creates an even narrower main beam but has a very high gain. By using eight of these arrays, the beamwidth can be increased and a much higher IPCG is obtained. The tradeoff is that more space is taken up on the board, but utilizing a multilayer substrate and proper design, we can reduce space requirement.

Another area for possible work would be to add beam forming technique, so that our rectenna can move its beam towards the source to ensure maximum power transfer. We will have to reduce the return loss for overall circuit, since power management is very important for this kind of power harvesting circuit.

Also, in future work other diodes such as Super diode and DC bias Schottky diode need to investigate using similar methodology to improve voltage sensitivity of the rectifier circuits.

Bibliography

1. *The History of Power Transmission by Radio Waves.* **William C. Brown, Fellow, IEEE.** september 1984, IEEE Transitions on Microwave Theory and Techniques, Vol.MTT-32, No.9.

2. wikipedia. [Online] http://en.wikipedia.org/wiki/Near_and_far_field.

3. *On the guided propagation of electromagnetic On the guided propagation of electromagnetic.* **Schwering., G. Goubau and F.** s.l. : IRE Trans. Antennas Propagat.,, Vols. Vol. AP-9:248–256, May 1961.

4. wikipedia. [Online] http://en.wikipedia.org/wiki/Free-space_path_loss.

5. RFcafe. [Online] http://www.rfcafe.com/references/electrical/atm-absorption.htm.

6. **Bourns.** *Chip Diode Application Note.* 2008.

7. *HSMS-2700, 2702, 270B, 270C, 270P High Performance Schottky Diode for Transient Suppression.*

8. *The Zero Bias Schottky Diode Detector at Temperature Extremes- Problems and Solutions Application Note 1090.*

9. *Zero Bias Detected RF/ID Market.* **Buted, Ronaldo R.**

10. *Wireless Transmission of Power for Sensors in Context Aware Spaces.* **Araiza, Jorge Ulises Martinez.**

11. *Effect of different substrates on Compact stacked square Microstrip Antenna.* **Asok De, N.S. Raghava, Sagar Malhotra, Pushkar Arora, Rishik Bazaz.** 1, s.l. : JOURNAL OF TELECOMMUNICATIONS, FEBRUARY 2010, Vol. 1.

12. *HSMS-286x Series Surface Mount Microwave Schottky Detector Diodes.* s.l. : Avago Technologies.

13. *HSMS-8101, 8202, 8207, 8209 Surface Mount Microwave Schottky Mixer Diodes.* s.l. : Avago Technologies.

14. *Electronic Devices and Circuit Theory. Prentice-Hall.* **Nashelsky., R. Boylestad and L.** 1987.

15. *Designing Detectors for RF/ID Tags ,Applcation Note 1089.*

16. *Hybrid Rectenna and Monolithic Integrated Zero-Bias Microwave Rectifier.* **Jamal Zbitou, Mohamed Latrach, Member, IEEE, and Serge Toutain.** s.l. : IEEE TRANSACTIONS ON MICROWAVE THEORY AND TECHNIQUES, JANUARY 2006, Vols. VOL. 54, NO. 1,.

17. *Wireless Transmission of Power for Sensors in Context Aware Spaces.* **Araiza, Jorge Ulises Martinez.**

18. *Fully Integrated Dickson Charge Pumps with Optimized Power Efficiency.* **Doutreloigne, Jan.** San Francisco, USA : Proceedings of the World Congress on Engineering and Computer Science 2010, October 20-22, 2010, Vol. 2.

19. **Coporation, ROGERS.** *RO4000® Series High Frequency Circuit Materials.*